Title: Cell Intrinsic Control of Death and Proliferation of Lymphocytes in Immune Response and Tumor Cells by pH

Wei-ping Zeng, Ph.D.[1,*]

[1]Therazwimm Corporation, 3128 Ferguson Road, Huntington, WV 25705

[*]Correspondence: Wei-ping Zeng, Therazwimm Corporation, 3128 Ferguson Road, WV 25705, USA. E-mail: weipingzengny@gmail.com.

Abstract

Many biological processes are controlled by cell death and proliferation. The present study found that intracellular pH positively correlated with proliferation but negatively with apoptosis. Acid treatments lowered intracellular pH and preferentially depleted highly proliferating lymphocytes, whereas alkaline treatments increased intracellular pH and enhanced lymphocyte proliferation. Likewise, acid treatments induced apoptosis and alkaline treatments maintained proliferation of tumor cells. These findings support a unified theory of regulation of cell death and proliferation where an intracellular pH balance controls both events, and the mitochondria act as the pH-stats of the cell. Accordingly, the Warburg effect is explained as necessary for proliferating cells to have a high intracellular pH environment to accelerate proliferation and avoid low pH-induced death.

Introduction

Cell death and proliferation play fundamental roles in numerous biological processes throughout the life cycle of an organism. In humans and animals, cell death and proliferation are key to understanding immune response and tumorigenesis, two biological processes that are of particular importance for the health of an individual. An immune response commences with clonal expansion of antigen specific lymphocytes and ends with the death of most of the expanded antigen specific lymphocytes by mitochondrion- and death receptor-initiated apoptosis. Death receptor-initiated apoptosis may also be linked to the mitochondrial processes. (Adachi et al., 1993; Burnet, 1959; Hildeman et al., 2002; Jost et al., 2009; Li et al., 1998; Liu et al., 1996; Luo et al., 1998). Unlike normal lymphocytes, tumor cells are characteristically resistant to death, and can endlessly proliferate. In many tumor cells, the genes for apoptosis inhibitors are over expressed or amplified whereas genes for apoptosis activators are suppressed or deleted. (Czabotar et al., 2014).

On the other hand, mammalian cell proliferation is primarily controlled at the "restriction point" by retinoblastoma family proteins (pRB). (Friend et al., 1986; Weinberg, 1995). Mitogenic signals generated by external stimulants at the cell membrane are transduced to the nucleus to induce the transcription of D and E type cyclin genes, which leads to the activation of the cyclin-dependent kinases CDK4/6 and CDK2, respectively. The activated CDKs phosphorylate the pRB proteins. (Akiyama et al., 1992; Ewen et al., 1993; Hinds et al., 1992; Kato et al., 1993). Phosphorylated pRB proteins dissociate with E2F family transcription factors to allow the latter to activate target gene expression, which drives the cell to pass the restriction point, transition from G1 to S phase and commit to completing the cell cycle. (Chellappan et al., 1991; Dyson et al., 1993).

Although apoptosis and G1/S transition appear to be controlled by separate pathways, the increased demand of energy and substrates for anabolic metabolism of the proliferating cells suggests that mitochondria may positively regulate both events. On the contrary, almost a century ago Otto Warburg observed that cell malignant transformation includes a precancerous phase, in which the cell must incur irreversible "injury of respiration" or "uncoupling of respiration and phosphorylation" and switch energy production to glycolysis that is followed by pyruvate fermentation and excretion of the fermentation waste product lactate. (Warburg, 1923; Warburg, 1956). This phenomenon has come to be known as the "Warburg Effect", and later found to be shared by both tumor and normal proliferating cells including lymphocytes. (Vander Heiden et al., 2009; Vaupel and Multhoff, 2021; Wang et al., 1976). However, the Warburg metabolism in the cytosol is not only inefficient for energy production, but also by itself does not contribute to anabolic metabolism. This is because in this pathway only 2 ATPs per glucose are produced as opposed to a net production of 32 ATPs by glycolysis followed by the TCA cycle and oxidative phosphorylation in the mitochondrion; all atoms in the glucose are converted to lactate that cannot be further used by the cell; and there is no net production of NADH or $FADH_2$ as potential reducing equivalents for biomass synthesis. (Stryer, 1995). Intriguingly, unlike originally suggested by Warburg, mitochondria in most tumor cells and normal proliferating cells are not "injured" but functional. (Potter et al., 2016; Vaupel and Multhoff, 2021). Given that most tumor microenvironments are poor in nutrients (Grasmann et al., 2019), it is puzzling why the inefficient Warburg metabolism predominates in the tumor cells.

This article presents evidence that supports a unified theory of cell fate determination in which an intracellular pH balance dictates whether a cell dies or proliferates, and the mitochondria act as the cell's "pH-stats" by positively and negatively regulating the amount of

protons in the cytosol through aerobic respiration and glutaminolysis, respectively. Thus, the Warburg effect or the limiting of mitochondrial energy production by aerobic respiration is viewed as necessary for proliferating cells to avoid low pH-induced death and have a high pH environment to accelerate proliferation.

Results

The current study stemmed from an unexpected observation of thymic atrophy in animals that had received a test compound prepared in an acidic solution. (Manuscript in preparation). Since thymus is one of a few organs in adults that maintain active cell proliferation, this observation led to the investigation of whether pH regulates immune responses by affecting lymphocyte survival and proliferation in the draining lymph nodes where immune responses to local antigen exposure take place.

Positive relationship between intracellular pH and lymphocyte proliferation

To determine whether there is a natural correlation between intracellular pH and proliferation, lymph node cells were labeled with CFSE, and cultured with either IL-2 alone or IL-2 and anti-CD3 antibodies for the study of T cell proliferation, or alternatively with either IL-4 alone or IL-4 and the B cell mitogen lipopolysaccharide (LPS) for the study of B cell proliferation. Lymphocyte proliferation was measured by the serial dilution of the CFSE signals after each cell division, whereas the intracellular pH was measured by the fluorescence intensity of the pH indicator pHrodo™ Red AM that inversely correlates with intracellular pH. Proliferating lymphocytes were detected even in cultures with IL-2 or IL-4 alone, indicating the pre-existence of proliferating cells prior to anti-CD3 or LPS stimulation. (Fig. 1a and b). As expected, proliferating cells ($CFSE^{lo}$) increased with concurrent decrease of non-proliferating

cells ($CFSE^{hi}$) after stimulation by anti-CD3 antibodies or LPS. Even the pre-existent proliferating cells underwent further divisions as evidenced by the decrease of their CFSE signals. (Fig. 1a and b). Importantly, the highly proliferating cells that had undergone more than 3 divisions were almost exclusively in the cell populations of high intracellular pH, whereas cells that had fewer than 3 divisions were in cell populations of low intracellular pH. (Fig. 1a and b). Thus, although proliferating cells were detected in both pH high and low populations, highly proliferating cells were enriched in the pH high populations.

To determine whether similar correlations exist during in vivo immune response, mice were i.p. sensitized and i.t. challenged with ovalbumin (OVA). Cells of the lung-draining nodes the mediastinal lymph nodes (MLNs) of the mice were sorted based on their intracellular pH, then analyzed for the expression of Ki-67. Ki-67 is a widely used, reliable marker of proliferating cells; its level of expression positively correlates with rRNA and DNA synthesis. (Darzynkiewicz et al., 2015). Similarly to the in vitro studies, higher percentages of the highly proliferative ($Ki\text{-}67^{hi}$) CD4, CD8 T cells and B cells were detected in the proliferating pH^{hi} than pH^{lo} cells. (Fig. 1c).

Effects of pH modifiers on the lymphocyte populations in the MLNs

OVA-sensitized and challenged mice were subject to treatments with saline or saline plus HOAc, HCl or NaOH, and MLNs were harvested 7 days after the initial challenge and treatment. The total numbers of MLN cells in the HOAc-treated mice were greatly reduced as compared with those in the control saline-treated mice. The numbers of total MLN cells in the HCl-treated mice were also significantly reduced but to lesser degrees. In contrast, treatment with NaOH increased the total MLN cells. (Fig. 2a). The differences in the total MLN cells were not due to

differences in Treg cell populations because there were similar percentages of Treg cells among the different treatment groups. (Manuscript in preparation).

The total MLN lymphocytes consisted of populations of relatively small sizes and low granularities (Lym1) and populations of larger sizes and higher granularities (Lym2). The combined percentages of Lym1 and Lym2 in the total MLN cells were similar in all treatment groups. However, while the relative proportions of Lym1 and Lym2 were similar among the saline, HCl and NaOH treatment groups, the proportion of the Lym1 was decreased whereas that of Lym 2 increased in the HOAc-treated mice. (Fig. 2b, upper). Lym2 consisted mostly of B lymphoblasts, (Fig. 2b, lower right), which indicated that B cells were less susceptible than T cells to depletion by HOAc. Indeed, the percentages of both CD4 and CD8 T cells in Lym2 were greatly reduced in the HOAc-treated mice, whereas they were similar among the saline, HCl, and NaOH treatment groups. (Fig. 2, lower right).

Within the Lym1, the percentage of CD8 T cells in the HOAc-treated mice was only about half of that in the saline-treated mice, the percentage of CD4 T cells was also lower but to lesser extent, but percentage of B cells was higher due to the decrease of the T cells. (Fig. 2b, lower left). This result shows again that B cells were less susceptible to depletion by HOAc than T cells. The percentages of CD4, CD8 T cells and B cells in the Lym1 of the HCl-treated mice were similar to those of the saline-treated mice. In the NaOH-treated mice, the percentages of CD4 and CD8 T cells were slightly decreased, whereas that of B cells was accordingly increased. (Fig. 2b, lower left).

Thus, acid treatments reduced, whereas alkaline treatment increased, the number of MLNs cells during an immune response in vivo. Depletion by HOAc was more pronounced than by HCl. T cells were more susceptible to the acid-induced depletion than B cells. Similar

depletion of lymphocytes by the acids were also observed in MLNs harvested at an earlier time of 3 days after the initial OVA challenge. (Suppl. Fig. 1a, b).

Effects of treatments with pH modifiers on lymphocyte proliferation in the MLNs

Overall, the Lym1 cells had relatively low Ki-67 expression therefore were of low proliferative statuses. Nonetheless, small numbers of Ki-67^{hi} cells were detected. The percentages of Ki-67^{hi} Lym1 cells were similar among saline- HOAc- or HCl-treated mice. (Fig. 2c). However, at the earlier time point of 3 days after initial OVA challenge, the percentages of both Ki-67^{hi} and Ki-67^{lo} Lym1 cells were dramatically reduced in the HOAc-treated mice, and to a lesser degree, the percentage of Ki-67^{hi} Lym1 cells was also reduced in the HCl-treated mice. (Suppl. Fig. 1c). Despite the relatively high percentage of B cells in the Lym1 of the HOAc-treated mice, the percentage of Ki-67^{hi} cells in the Lym1 B cells was lower than in the saline-treated mice. The reduction, albeit smaller, was also observed in the HCl-treated mice. (Fig. 2c). Similar results were also observed at the earlier time point. (Suppl. Fig. 1c). In contrast to the acid treatments, NaOH treatments increased the percentages of Ki-67^{hi} Lym1 and Lym1 B cells. (Fig. 2c).

The Lym2 populations were more proliferative than the Lym1 populations. HOAc treatments decreased the percentages of Ki-67^{hi} Lym2 and Lym2 B cells. (Fig. 2c). Although the percentages of Ki-67^{hi} cells in Lym2 and Lym2 B cells of the HCl–treated mice were similar to those of the saline-treated mice, their Ki-67 mean fluorescence intensities were much lower than their counterparts in the saline-treated mice. (Fig. 2d). Therefore, like HOAc, HCl also negatively regulated cell proliferation. In contrast, NaOH treatments increased the percentages of Ki-67^{hi} Lym2 and Lym2 B cells. (Fig. 2c). At the earlier time point of 3 days after the initial OVA challenge, reductions of the percentages of Ki-67^{hi} cells of Lym2 and Lym2 B cells

were observed in both the HOAc- and HCl-treated mice with more reduction in the HOAc-treated mice. (Suppl. Fig. 1c).

Effects *of in vitro treatments with pH modifiers on proliferating lymphocytes*

Due to the complexity of the in vivo environment, it cannot be definitively determined whether the effects of the in vivo treatments with the pH modifiers on MLN lymphocytes were direct or indirect. Further, the fluidity of the in vivo environment could mask the full effects of the pH modifiers. For example, circulating and/or newly activated lymphocytes could replenish the MLNs after the depletion of the T cells by the acid treatments. Moreover, the kinetics of absorption and the subsequent transportation of the pH modifiers into and out of the MLNs are unknown. As such, the actual durations and concentrations of the pH modifiers at which the pH modifiers acted on the lymphocytes in the MLNs could not be determined.

To bypass these complexities and better assess the full potentials of the pH modifiers, in vitro experiments were carried out, in which primary MLN cells were treated with saline or saline plus the pH modifiers in FBS in a 37°C water bath. Such in vitro cultures were designed to be free of interference by pH buffering agents in common tissue culture system. The in vitro treatments with HCl or HOAc eliminated almost all Ki-67^{+} cells in total lymphocytes, CD4, CD8 T cells and B cells. In contrast, the in vitro treatment with NaOH more than tripled the percentages of Ki-67^{+} cells in the total lymphocytes and CD8 T cells, and nearly tripled in the CD4 T cells and B cells. (Fig. 3). Thus, the in vitro results collaborated the results of the in vivo treatments that acid treatments preferentially depleted, whereas alkaline treatment increased, the proliferating lymphocytes. The in vitro treatments showed stronger effects than the in vivo treatments, which was likely due to higher concentration and longer time of action of the pH modifiers in the in vitro cultures than in the MLNs in vivo.

Correlation between low intracellular pH and lymphocyte apoptosis

Having demonstrated a positive relationship between high pH and the rate of lymphocyte proliferation, further experiments were performed to determine whether conversely low pH correlates with lymphocyte death by apoptosis. In steady-state peripheral lymphocytes of unimmunized mice, about 5% of the total lymphocytes were apoptotic, and a similar percentage of the cells were early apoptotic (Annexin V^{hi} 7-AAD^{-}) (see (Vermes et al., 1995) for the definition of early apoptotic cells); these two populations were found in CD4, CD8 T cells and B cells. (Fig. 4a). Since direct measurement of intracellular pH of apoptotic (dead) cells was impossible because of their leaky cell membranes, early apoptotic cells were analyzed as proxies. In all live lymphocyte populations, the early apoptotic cells were detected primarily in cells of low intracellular pH. (Fig. 4b). In the MLNs of mice sensitized and challenged with OVA, small percentages of apoptotic cells were detected in total lymphocytes, CD4, CD8 T cells and B cells in all groups treated with saline or saline plus HOAc, or NaOH. (Fig. 4c). Similar to the steady-state lymphocytes, cells of low intracellular pH were enriched with early apoptotic cells (Annexin V^{hi} live cells). (Fig. 4d). Although early apoptotic cells were also detected in cells of relatively high pH (in Q1 quadrants in Fig. 4d), these early apoptotic cells had lower pH than their non-apoptotic counterparts (in Q4 quadrants) as judged by their higher mean fluorescence intensities of the pH indicator. (Fig. 4e). Apoptosis was also detected in lymphocytes from in vitro cultures stimulated by anti-CD3 antibodies or LPS, (Suppl. Fig. 2a, c) and early apoptotic cells were predominantly detected in the populations of low intracellular pH. (Suppl. Fig. 2b, d).

Increase of apoptosis by acid treatments

Although MLN cells were dramatically reduced by treatments with acids, particularly HOAc, (Fig. 2a; Suppl. Fig. 1a), percentage of apoptotic cells in ex vivo MLNs of HOAc-treated

mice was similar to that of saline-treated mice (Fig. 4c), which showed that apoptotic cells are quickly removed during the immune response in vivo (Nagata, 2018). Therefore, the effects of pH modifiers on apoptosis would be better assessed by in vitro experiments. After the MLN cells were treated with HOAc, more than 70% were apoptotic, whereas there were only 1.35% and 2.43% apoptotic cells after in vitro saline or NaOH treatment, respectively. (Fig. 5a). However, regardless of the treatments, early apoptotic cells were found primarily in the pH low populations. (Fig. 5b). Similar results were obtained with lymphocytes stimulated with anti-CD3 or LPS in vitro. (Suppl. Fig. 2).

Effects of treatments with pH modifiers on tumor cell viability and proliferation

Cell proliferation is a common feature of immune response and tumorigenesis. To determine weather the pH modifiers would have effects on tumor cells similar to those on proliferating normal lymphocytes, the human T and B cell tumor cell lines Jurkat and Raji, respectively, were treated with saline or saline plus HOAc or NaOH in FBS. Compared with saline treatment, HOAc treatment greatly reduced the viabilities of the Jurkat and Raji cells, whereas NaOH treatment only slightly decreased the viabilities. (Fig. 6a). The effects of HCl treatments were similar to those of the HOAc treatments. (Suppl. Fig. 3). The tumor cells were further analyzed for Ki-67 expression. After saline treatment, the majority of live Jurkat cells remained Ki-67^{+}. However, few, if any, (<2%) live Jurkat cells after the HOAc treatment were Ki-67^{+}. In contrast, the percentage of Ki-67^{+} live Jurkat cells after NaOH treatment was similar to that after saline treatment. In Raji cells, HOAc treatment dramatically reduced the percentage of Ki-67^{hi} cells as compared with saline treatment. In contrast, the percentage of Ki-67^{hi} Raji cells after NaOH treatment was similar to that after saline treatment. (Fig. 6b). These results

demonstrated that the proliferative statuses of the tumor cells are positively correlated with their susceptibilities to depletion by the acid treatments.

Low pH correlated with tumor cell apoptosis

The tumor cells were also analyzed for apoptosis and intracellular pH. High percentages of apoptotic Jurkat and Raji cells were detected in all treatment groups. (Fig. 6c and d, upper panels). The percentages of apoptotic cells detected in the saline and NaOH treatment groups were much higher than the percentages of death cells determined in the viability tests by Trypan blue staining in Fig. 6a. This was likely due to additional apoptotic cell death caused by the removal of the tumor cells from the FBS and incubation in serum free buffers at 37°C and room temperature during staining with the pH indicator and Annexin V. Conversely, many cells that had died earlier in the HOAc treatment groups had disintegrated during the staining processes. Nonetheless, regardless of the treatments, early apoptotic cells were enriched in tumor cell populations of low intracellular pH. (Fig. 6c and d, lower panels). Although early apoptotic cells were also found in the pH^{hi} Jurkat cell populations, these pH "high" early apoptotic cells had stronger staining of the pH indicator hence lower pH than their non-apoptotic pH^{hi} counterparts. (Fig. 6c, lower panels).

Treatments with pH modifiers altered intracellular pH

Thus, the effects of treatments with the pH modifiers on lymphocytes and tumor were consistent with the natural correlations between intracellular pH and cell proliferation and death. However, the question remained whether the treatments could alter intracellular pH. To answer this question, MLN cells of mice sensitized and challenged with OVA were stained for intracellular pH and surface markers. Jurkat and Raji cells were stained for intracellular pH only. The stained cells were divided for treatments with saline or saline plus HOAc or NaOH in FBS.

In anticipation of more cell loss due to acid treatments, more stained cells were used for HOAc treatments than for saline or NaOH treatments in the studies of the MLN T cells and tumor cells. After the treatments, live and dead cells were distinguished by 7AAD staining. Flow cytometry analysis of the intracellular pH confirmed that HOAc treatments decreased whereas NaOH treatments increased intracellular pH, respectively, in live total MLN lymphocytes, B cells, CD4 and CD8 T cells. (Fig. 7a). Similar changes were also observed in Jurkat and Raji cells. (Fig. 7b).

Discussion

This article investigates the impact of pH on the survival and proliferation of normal lymphocytes in an active immune response and in tumor cells. It was found that the rate of cell proliferation is positively whereas apoptosis is negatively correlated with intracellular pH. Therefore, it appears that an intracellular pH balance dictates whether a cell accelerates proliferation or dies. When the pH balance tips higher, proliferation increases, when it tips lower, the cell may die. In agreement, alkaline treatments increased intracellular pH and enhanced cell proliferation whereas acid treatments decreased intracellular pH and induced apoptosis. The susceptibility to acid-induced death was determined in part by the cell's proliferative status. Highly proliferative cells were more susceptible than modestly proliferating cells, which in turn were more susceptible than non-proliferating cells.

Mitochondria are likely the main regulators of intracellular pH. Mitochondria are the main organelles that can cause net increase of protons in the cells during the production of energy through aerobic respiration. Catabolizing 1 glucose molecule through glycolysis and mitochondrial pathways produces 6 CO_2, 10 ($NADH + H^+$) and 2 $FADH_2$. CO_2 is converted to

carbonic acids in the cell by carbonic anhydrase, which produces protons. (Meldrum and Roughton, 1933; Tripp et al., 2001). On the other hand, NADH is fed to the electron transport chain (ETC) to create mitochondrial membrane potential and proton gradient to drive ATP synthesis. However, up to 20 to 25% of mitochondrial respiration is uncoupled from ATP synthesis, which can also cause net increases of protons in the cell that can spill across the mitochondrial outer membrane to the cytosol. (Fantin et al., 2006; Rolfe and Brown, 1997). In addition to the ETC, ATP synthase can also transport protons in reverse direction from mitochondrial matrix to the intermembrane space especially when the ATP/ADP ratio is high. (Baffy, 2017). Consequently, if mitochondrial respiration were to increase without restriction to meet the heightened energy demand of proliferating cell, it would be incompatible with a high intracellular pH environment for high proliferation, but instead tip the intracellular pH balance lower to trigger apoptosis.

Indeed, instead of mitochondrial respiration, glycolysis in the cytosol and glutaminolysis in the mitochondria are characteristic of energy metabolism in proliferating cells. Glycolysis followed by lactate excretion produces no CO_2 and no net NADH + H^+ and $FADH_2$, whereas in glutaminolysis, glutamine is deaminated to produce ammonia and glutamate. As found in many tumor cells, glutamate is often excreted from proliferating cells, (LeBoeuf et al., 2020), which together with ammonia production can increase intracellular pH. Glutamate can also be further metabolized and participate in the malate-aspartate shuttle to move protons from cytosol to mitochondria by the actions of malate dehydrogenases to raise cytosolic pH. Thus, the Warburg effect could be the strategy of highly proliferating cells to satisfy the requirement for high intracellular pH for high proliferation and to avoid low pH-induced death.

The Warburg effect is evolutionary conserved as similar phenomena are observed across species. For example, yeast growth accelerates as glucose concentration increases. However, when the yeast growth and glucose concentration reach critical points, the yeasts switch energy production from aerobic respiration to fermentation. This phenomenon is known as Crabtree effect. (Pfeiffer and Morley, 2014; Ziv et al., 2013). It is conceivable that the switch is necessary for the yeasts' survival because if aerobic respiration continues to increase, it could lower intracellular pH to induce cell death. In bacteria, the Entner-Doudoroff glycolytic pathway is inefficient for energy production, but counter intuitively it is much more common among aerobic and facultative than anaerobic bacteria, suggesting that this pathway is needed to substitute for aerobic respiration for bacterial survival. (Flamholz et al., 2013). Indeed, like the yeasts, bacteria switch to energetically inefficient metabolism when growth rate increases to a critical level. (Vemuri et al., 2006). Parasites also appear to adopt similar strategy during the stages of their life cycles in mammalian hosts. (Homewood, 1977; Moyersoen et al., 2004; You et al., 2014). Such evolutionary conservation suggests that pH modifiers can be used to control not only immune response and tumorigenesis as shown in this study but also the survival and proliferation of pathogens regardless of their abilities to resist currently available anti-microbial drugs.

The finding that low proliferating cells had low pH whereas highly proliferating cells have high pH may reflect the dynamic links between lymphocyte proliferation and metabolism. Under the pH balance theory proposed in this article, it is expected that at low rates of proliferation lymphocytes may only need to use mitochondrial respiration to generate energy. When the proliferation rate increases, as a result of cumulative or synergic effects of antigen stimulation, co-stimulation and growth factors, lymphocytes may increase Warburg metabolism

to avoid overuse of mitochondrial respiration that could lead to intracellular acidification and consequently cell death. Not only this principle provides a new perspective for understanding the clonal expansion phase of an immune response, it may also be key to understanding the culling of activated lymphocytes and transition to memory cells at the end of an immune response. Conceivably, as the signals for sustaining Warburg metabolism and glutaminolysis in the clonal expansion phase subside, lymphocytes that remain highly proliferative would be forced to overuse mitochondrial respiration to meet high energy demand so that become self-destructive. In contrast, lymphocytes that have lowered their proliferative propensity or developed new mechanisms to sustain adequate Warburg metabolism and glutaminolysis would avoid the overuse of mitochondrial respiration thereby survive to become memory cells.

From a clinical perspective, data presented here can be basis for rational design of new therapies aiming to either enhance or suppress immune and/or inflammatory responses. In situations such as cancers and infectious diseases where there is insufficient protective immunity, pH modifiers that increase or resist the fall of pH could be used to promote lymphocyte proliferation therefore enhance protective immunity. In other situations where overzealous immune or inflammatory responses impair normal tissue structure and functions, pH modifiers that decrease pH or resist the rise of pH may be used to dampen the overzealous immune or inflammatory responses. Such treatments could also suppress tissue cell hyperplasia that often accompanies inflammation.

The present study also provides new insights into the role of pH in tumorigenesis. A previous study found that acidic tumor microenvironment (TME) promotes tumor cell invasion of local tissue. (Estrella et al., 2013). Therefore, it is believed that acidic environment is favorable for tumorigenesis, and neutralizing the acidic TME by alkaline treatment is proposed

as anti-tumor therapy. (Corbet and Feron, 2017). However, according to the present study, low pH is unfavorable to tumor cell proliferation and could induce apoptosis. Thus, contrary to the previous view, the present study shows that lowering rather than raising pH could be a potentially new anti-tumor therapy by directly inducing tumor cell apoptosis. Lowering pH could be achieved by inducing the accumulation of protons in the tumor cells through overactive mitochondrial respiration or inhibiting the export of protons to the extracellular space or the import of bicarbonate or other alkaline substances to the cells. Alternatively, lowering pH could be achieved through exogenous reduction of pH in tumor extracellular space, for example by acid treatment as in this study, which overpowers the tumor cells' ability to maintain pH homeostasis. Since small molecule pH modifiers such as acids can permeate all tissues, they could be particularly effective anti-tumor agents at the early or metastatic phases of tumorigenesis when the tumor cells are difficult to locate. In contrast, alkaline treatment carries an inherent risk of increasing tumor cell proliferation. However, patients could benefit from its enhancement of proliferation of anti-tumor immune cells.

Apart from the cell's proliferative status, cell types affect their responses to pH modifiers. For example, B cells in the MLNs were found less susceptible to acid-induced depletion than T cells. The exact mechanisms for the difference is unknown, but could be attributable to their different expression and/or activities of the enzymes and membrane transporters responsible for pH homeostasis, or their different anatomical distribution in the lymph nodes. Further, different pH modifiers of the same class could have varied effects on the same cells. For example, HOAc was found to have stronger effects than HCl in inducing lymphocyte death in the MLNs. Furthermore, the stronger effects of in vitro treatments with pH modifiers than in vivo treatments showed that the concentration of pH modifiers and the duration of treatment are also important

factors that determine the potency of the pH modifiers. These features can be exploited to selectively target pathological cells or protective normal cells for the treatment and prevention of diseases whose pathogenesis is in part or in full attributed to cell proliferation.

As indicated in the foregoing, pH modifiers for disease treatment and prevention can include not only acids, bases and pH buffering agents, but also ionophores, and inhibitors and stimulators of the expression and/or activities of enzymes (e.g., carbonic anhydrases), membrane transporters (e.g., monocarboxylate transporters, Na^+/H^+ exchangers) and ion channels that are responsible for the maintenance and change of pH in and around a cell.

Finally, although it is generally believed that the pH in a human or animal is maintained at a stable level of about 7.40, humans can experience transient severe acidosis without serious pathological consequences in the aftermath. (Bangsbo et al., 1993; Hopkins and Sharma, 2019; Orringer et al., 1977). In the present study, administration of pH modifiers was well tolerated by the animals. Therefore, disease treatments and prevention with pH modifiers can be reasonably expected to be well tolerated by human and animal subjects.

Figure Legends

Fig. 1. Positive correlation between intracellular pH and lymphocyte proliferation.

(a) CFSE-labeled lymph node cells stimulated in vitro with IL-2, or IL-2 and anti-CD3 antibodies. Shown are flow cytometric pseudocolor plots of CFSE signals and intracellular pH, and histograms of CFSE signals of live total lymphocytes, CD4, CD8 T cells and B cells.

(b) CFSE-labeled lymph node cells stimulated in vitro with IL-4 or IL-4 and LPS.

(c) Draining lymph node cells of in vivo immune response. OVA-sensitized mice were i.t. challenged with OVA every other day for 3 time, and MLNs were harvested 7 days after the

initial challenge. Live MLN cells were sorted into pH high and low populations. Left panels are the histograms of the intracellular pH profiles of the sorted populations. Right panels are histograms of Ki-67 expression showing the percentages of Ki-67 high and low cells in the proliferating CD4, CD8 T cells and B cells ($CD19^+$) of the sorted populations.

Fig. 2. Effects of pH modifiers on the populations and proliferation of lymphocytes in MLNs.

(a) Total numbers of MLN cells. Upper: Schematic illustration of the schedules for OVA challenges and treatments with saline, or saline plus HCl, HOAc or NaOH of the OVA-sensitized mice. Arrows indicate the time points for the challenges or treatments. Lower: A graph showing the average total numbers of MLN cells of mice in the different treatment groups. Statistical significance between the saline and the other groups was determined by Student t test; * $p < 0.05$, ** $p < 0.01$.

(b) Lymphocyte populations in the MLNs. The upper panels are flow cytometry plots showing the Lym1 and Lym2 lymphocyte populations in live MLN cells of the different treatment groups. The lower panels show the populations of CD4, CD8 T cells and B cells ($CD19^+$) in Lym1 and Lym2. Numbers in the plots are the percentages of each cell populations.

(c) Expression of Ki-67. Left panels are histograms showing Ki-67 expression, and the percentages of Ki-67 high, low negative cells in Lym1, Lym2 and B cells thereof. Right panels are graphic presentation of the percentages of the Ki-67 high and low cells in the left panels.

(d) Mean fluorescence intensities of Ki-67^{hi} cells in the Lym2 populations and their B cells of the different treatment groups.

Fig. 3. Effects of in vitro treatments with pH modifiers on lymphocyte proliferation. Primary lymph node cells were incubated in FBS containing 10% saline or saline plus HCl, HOAc or NaOH, then analyzed by flow cytometry to determine Ki-67 expression in live total lymphocytes, CD4, CD8 T cells and B cells ($CD19^+$). Left panels are histograms of Ki-67 expression in the different lymphocyte populations. Right panel is graphic presentation of the percentages of $Ki\text{-}67^+$ cells in the left panels.

Fig. 4. Relation between low intracellular pH and lymphocyte apoptosis. Total lymphocytes, CD4, CD8 T cells and B cells under different experimental conditions as indicated were analyzed by flow cytometry for the staining of Annexin V, 7AAD or Zombie-violet, and the pH indicator pHrodo™ Green. (a, b) Steady-state peripheral lymphocytes of unimmunized mice.

(a) Plots showing the staining of Annexin V and 7AAD. Cells in the Q2 quadrants (Annexin V^{hi} $7AAD^+$) are apoptotic cells, and cells in the Q3 quadrants (Annexin V^{hi} $7AAD^{-)}$ are early apoptotic cells.

(b) Plots showing the staining of pH indicator and Annexin V in live ($7AAD^-$) populations of the different lymphocytes as indicated.

(c, d, e) Ex vivo MLN cells of OVA-sensitized and challenged mice that were treated with saline or saline plus HOAc or NaOH as indicated.

(c) Plots showing the staining of Annexin V and Zombie-violet of the different lymphocytes as indicated.

(d) Plots showing the staining of Annexin V and the pH indicator in live populations (Zombie-$violet^-$) of the different lymphocytes.

(e) Bar graphs showing the mean fluorescence intensities (MFI) of pHrodo™ Green of the early apoptotic (Annexin V^{hi}) cells (Q1) and the non-apoptotic (Annexin V^{lo}) cells (Q4) within the pH high cells in (d).

Fig. 5. Effects of in vitro treatments with pH modifiers on apoptosis of MLN lymphocytes. MLN cells from mice that were sensitized and challenged with OVA were treated in vitro with saline or saline plus HOAc or NaOH in FBS.

(a) Plots showing the staining of 7AAD and Annexin V in total lymphocytes, CD4, CD8 T cells and B cells in the different treatment groups.

(b) Plots showing the staining of the pH indicator and Annexin V in live total lymphocytes, CD4, CD8 T cells and B cells.

Fig. 6. Effects of pH modifiers on the proliferation and apoptosis of tumor cells.

(a) Comparison of the average viabilities of Jurkat and Raji cells as determined by Trypan Blue staining after treatments with saline or saline plus HOAc or NaOH in FBS. Statistical significance of differences between the saline and other treatment groups was determined by Student t test, * $p < 0.05$, ** $p < 0.01$.

(b) Histograms of Ki-67 staining in live Jurkat or Raji cells after the different treatments. The numbers in the histograms are the percentages of each population defined by their levels of Ki-67 staining.

(c) Apoptosis of Jurkat cells. Upper panels show the staining of 7AAD and Annexin V of Jurkat cells after the different treatments. Lower panels show the staining of the pH indicator and Annexin V in live ($7AAD^-$) Jurkat cells after the treatments.

(d) Apoptosis of Raji cells. Upper panels show the staining of 7AAD and Annexin V of Raji cells after the different treatments. Lower panels show the staining of the pH indicator and Annexin V in live Raji cells after the treatments.

Fig. 7. Alteration of intracellular pH by treatments with pH modifiers.

(a) MLN cells of OVA-sensitized and challenged mice. Sensitizations, challenges and MLN collection were carried out as in Fig. 1c. MLN cells were treated in vitro as indicated. Shown are overlays of histograms of intracellular pH of the different lymphocyte populations of after the treatments. MFI: mean fluorescence intensity of pHrodo™ Green staining.

(b) Jurkat and Raji cells. Shown are overlays of histograms of intracellular pH after the different treatments.

Materials and Methods

Mice

Balb/c female mice were purchased from Jackson Laboratory (Bar Harbor, ME) and housed in the animal facility of Charles River Accelerator and Development Lab (CRADL) (Cambridge, MA). Animal studies were performed according to the protocols approved by the CRADL Institutional Animal Care and Use Committee.

CFSE labeling and activation of lymph node cells

Lymph node cells were washed 3 times with plain PBS. After the wash, the cells (3-5 x 10^6/ml) were incubated in 1μm Carboxyfluorescein succinimidyl ester (CFSE) (Fluka/Sigma-Aldrich, Burlington, VT) in plain PBS at room temperature for 7 minutes. After the incubation, 1/4 volume of FBS was added to stop the labeling, and cells were washed 4 times with PBS plus

1% FBS. The labeled cells were cultured with IL-2 (20 units/ml) or IL-2 plus anti-CD3 antibody (1μg/ml) (BD Pharmingen (San Diego, CA). Alternatively, the labeled cells were cultured with IL-4 (4ng/ml) or IL-4 plus lipopolysaccharide (LPS) (10μg/ml) (Sigma-Aldrich, St. Louis, MO). Two and half days later, cells were harvested for further experiments.

Measuring intracellular pH

The intracellular pH indicators pHrodo™ Green/Red AM were purchased from ThermoFisher Scientific (Waltham, MA). Intracelluar pH of lymphocytes was measured according to the manufacture's instructions. Briefly, cells were washed once with Live Cell Image Solution (LCIS) (Life Technoology/ThermoFisher Scientific, Grand Island, NY). Immediately prior to use, the pH indicator pHrodo™ Greenn/Red AM and the PowerLoad were mixed then diluted in the LCIS to produce working solution containing 0.5-1μM pH indicator. The cells (1-2 x 10^7/ml) were suspended in the working solution and incubated in a 37°C water bath for 30 minutes. After the incubation, the cells were washed once in LCIS containing 1% FBS, and stained with Zombie-Violet viability dye or 7AAD. (Biolegend, San Diego, CA). Fluorescence emitted by the pH indicators in live cells (Zombie or 7AAD negative) was detected by flow cytometry.

OVA sensitization, challenge and treatments of mice

OVA sensitization and challenge were performed as previously described. (Rangasamy et al., 2005; Zeng et al., 2017). Briefly, Balb/c mice were sensitized by i.p. injection of 20μg OVA (Sigma-Aldrich, St. Louis, MO) plus Alum adjuvant (Thermo Scientific, Rockford, IL). Two weeks later, the sensitization is repeated with 500μg OVA. About two weeks later, mice were challenged with 100μg OVA in 60μl saline by intratracheal (i.t.) instillation, and the challenges were repeated as described in each experiment. For treatments, mice received i.t. instillation of

60μl saline or saline containing 175mM HOAc or HCl along with OVA challenge. Since mice were less tolerant to i.t. instillation of NaOH, NaOH treatments were carried out by i.p. injection of 200μl of saline containing 87.5mM NaOH. After the challenges and treatments, mediastinal lymph nodes were collected at the times specified in the different experiments.

In vitro treatments of lymphocytes and tumor cells

Lymph node cells (4 x 10^6 cells/ml) were incubated in FBS containing 10% of saline or saline plus 87.5mM HCl, HOAc or NaOH in 37°C water bath for 5 hours before analyses. The Jurkat and Raji cells (2 x 10^6 cells/ml) were incubated in FBS containing 10% saline or 87.5mM HCl, HOAc or NaOH prepared in saline in 37°C water bath for 3-5 hours.

Flow cytometry

Fluorochrome-conjugated anti-mouse antibodies against CD3, CD4, CD8, CD19 and Ki-67, Zombie-Green and Zombie-Violet fixable viability dyes and Foxp3 buffer set were purchased from Biolegend (San Diego, CA). Lymphocytes were first stained with Zombie viability dye, followed by staining for cell surface marker CD4, CD8 and CD19. The cells were then fixed with CytoFix/CytoPerm buffer, washed with PBS plus 1% FBS and 1x CytoPerm buffer, and stained for Ki-67. Jurkat and Raji cells were stained with Zombie-Green dye followed by fixation, permealization and staining with anti-human Ki-67. (Biolegend, San Diego, CA). For Annexin V staining, cells were washed twice with plain PBS and once with Annexin V binging buffer (10mM HEPES, pH7.4, 140mM NaCl, 2.5mM $CaCl_2$) and incubated with fluorochrome-conjugated Annexin V in Annexin V binding buffer for 15min at room temperature. The cells were washed twice in Annexin V binding buffer, and resuspended in Annexin V binding buffer. 7-AAD was added to the cells before analyzed by flow cytometry.

References

Adachi, M., Watanabe-Fukunaga, R., and Nagata, S. (1993). Aberrant transcription caused by the insertion of an early transposable element in an intron of the Fas antigen gene of lpr mice. Proc Natl Acad Sci U S A *90*, 1756-1760.

Akiyama, T., Ohuchi, T., Sumida, S., Matsumoto, K., and Toyoshima, K. (1992). Phosphorylation of the retinoblastoma protein by cdk2. Proc Natl Acad Sci U S A *89*, 7900-7904.

Baffy, G. (2017). Mitochondrial uncoupling in cancer cells: Liabilities and opportunities. Biochim Biophys Acta Bioenerg *1858*, 655-664.

Bangsbo, J., Johansen, L., Graham, T., and Saltin, B. (1993). Lactate and H+ effluxes from human skeletal muscles during intense, dynamic exercise. J Physiol *462*, 115-133.

Burnet, F. (1959). The Clonal Selection Theory of Acquired Immunity (London: Cambridge University Press).

Chellappan, S.P., Hiebert, S., Mudryj, M., Horowitz, J.M., and Nevins, J.R. (1991). The E2F transcription factor is a cellular target for the RB protein. Cell *65*, 1053-1061.

Corbet, C., and Feron, O. (2017). Tumour acidosis: from the passenger to the driver's seat. Nat Rev Cancer *17*, 577-593.

Czabotar, P.E., Lessene, G., Strasser, A., and Adams, J.M. (2014). Control of apoptosis by the BCL-2 protein family: implications for physiology and therapy. Nat Rev Mol Cell Biol *15*, 49-63.

Darzynkiewicz, Z., Zhao, H., Zhang, S., Lee, M.Y., Lee, E.Y., and Zhang, Z. (2015). Initiation and termination of DNA replication during S phase in relation to cyclins D1, E and A, p21WAF1, Cdt1 and the p12 subunit of DNA polymerase delta revealed in individual cells by cytometry. Oncotarget *6*, 11735-11750.

Dyson, N., Dembski, M., Fattaey, A., Ngwu, C., Ewen, M., and Helin, K. (1993). Analysis of p107-associated proteins: p107 associates with a form of E2F that differs from pRB-associated E2F-1. J Virol *67*, 7641-7647.

Estrella, V., Chen, T., Lloyd, M., Wojtkowiak, J., Cornnell, H.H., Ibrahim-Hashim, A., Bailey, K., Balagurunathan, Y., Rothberg, J.M., Sloane, B.F.*, et al.* (2013). Acidity generated by the tumor microenvironment drives local invasion. Cancer Res *73*, 1524-1535.

Ewen, M.E., Sluss, H.K., Sherr, C.J., Matsushime, H., Kato, J., and Livingston, D.M. (1993). Functional interactions of the retinoblastoma protein with mammalian D-type cyclins. Cell *73*, 487-497.

Fantin, V.R., St-Pierre, J., and Leder, P. (2006). Attenuation of LDH-A expression uncovers a link between glycolysis, mitochondrial physiology, and tumor maintenance. Cancer Cell *9*, 425-434.

Flamholz, A., Noor, E., Bar-Even, A., Liebermeister, W., and Milo, R. (2013). Glycolytic strategy as a tradeoff between energy yield and protein cost. Proc Natl Acad Sci U S A *110*, 10039-10044.

Friend, S.H., Bernards, R., Rogelj, S., Weinberg, R.A., Rapaport, J.M., Albert, D.M., and Dryja, T.P. (1986). A human DNA segment with properties of the gene that predisposes to retinoblastoma and osteosarcoma. Nature *323*, 643-646.

Grasmann, G., Smolle, E., Olschewski, H., and Leithner, K. (2019). Gluconeogenesis in cancer cells - Repurposing of a starvation-induced metabolic pathway? Biochim Biophys Acta Rev Cancer *1872*, 24-36.

Hildeman, D.A., Zhu, Y., Mitchell, T.C., Kappler, J., and Marrack, P. (2002). Molecular mechanisms of activated T cell death in vivo. Curr Opin Immunol *14*, 354-359.

Hinds, P.W., Mittnacht, S., Dulic, V., Arnold, A., Reed, S.I., and Weinberg, R.A. (1992). Regulation of retinoblastoma protein functions by ectopic expression of human cyclins. Cell *70*, 993-1006.

Homewood, C.A. (1977). Carbohydrate metabolism of malarial parasites. Bull World Health Organ *55*, 229-235.

Hopkins, E., and Sharma, S. (2019). Acid Base Balance. In Physiology (NCBI Bookshelf: StatPearls Publishing).

Jost, P.J., Grabow, S., Gray, D., McKenzie, M.D., Nachbur, U., Huang, D.C., Bouillet, P., Thomas, H.E., Borner, C., Silke, J.*, et al.* (2009). XIAP discriminates between type I and type II FAS-induced apoptosis. Nature *460*, 1035-1039.

Kato, J., Matsushime, H., Hiebert, S.W., Ewen, M.E., and Sherr, C.J. (1993). Direct binding of cyclin D to the retinoblastoma gene product (pRb) and pRb phosphorylation by the cyclin D-dependent kinase CDK4. Genes Dev *7*, 331-342.

LeBoeuf, S.E., Wu, W.L., Karakousi, T.R., Karadal, B., Jackson, S.R., Davidson, S.M., Wong, K.K., Koralov, S.B., Sayin, V.I., and Papagiannakopoulos, T. (2020). Activation of Oxidative Stress Response in Cancer Generates a Druggable Dependency on Exogenous Non-essential Amino Acids. Cell Metab *31*, 339-350 e334.

Li, H., Zhu, H., Xu, C.J., and Yuan, J. (1998). Cleavage of BID by caspase 8 mediates the mitochondrial damage in the Fas pathway of apoptosis. Cell *94*, 491-501.

Liu, X., Kim, C.N., Yang, J., Jemmerson, R., and Wang, X. (1996). Induction of apoptotic program in cell-free extracts: requirement for dATP and cytochrome c. Cell *86*, 147-157.

Luo, X., Budihardjo, I., Zou, H., Slaughter, C., and Wang, X. (1998). Bid, a Bcl2 interacting protein, mediates cytochrome c release from mitochondria in response to activation of cell surface death receptors. Cell *94*, 481-490.

Meldrum, N.U., and Roughton, F.J. (1933). Carbonic anhydrase. Its preparation and properties. J Physiol *80*, 113-142.

Moyersoen, J., Choe, J., Fan, E., Hol, W.G., and Michels, P.A. (2004). Biogenesis of peroxisomes and glycosomes: trypanosomatid glycosome assembly is a promising new drug target. FEMS Microbiol Rev *28*, 603-643.

Nagata, S. (2018). Apoptosis and Clearance of Apoptotic Cells. Annu Rev Immunol *36*, 489-517.

Orringer, C.E., Eustace, J.C., Wunsch, C.D., and Gardner, L.B. (1977). Natural history of lactic acidosis after grand-mal seizures. A model for the study of an anion-gap acidosis not associated with hyperkalemia. N Engl J Med *297*, 796-799.

Pfeiffer, T., and Morley, A. (2014). An evolutionary perspective on the Crabtree effect. Front Mol Biosci *1*, 17.

Potter, M., Newport, E., and Morten, K.J. (2016). The Warburg effect: 80 years on. Biochem Soc Trans *44*, 1499-1505.

Rangasamy, T., Guo, J., Mitzner, W.A., Roman, J., Singh, A., Fryer, A.D., Yamamoto, M., Kensler, T.W., Tuder, R.M., Georas, S.N., *et al.* (2005). Disruption of Nrf2 enhances susceptibility to severe airway inflammation and asthma in mice. J Exp Med *202*, 47-59.

Rolfe, D.F., and Brown, G.C. (1997). Cellular energy utilization and molecular origin of standard metabolic rate in mammals. Physiol Rev *77*, 731-758.

Stryer, L. (1995). Biochemistry, 4th edn (New York – Basingstoke: W. H. Freeman and Company).

Tripp, B.C., Smith, K., and Ferry, J.G. (2001). Carbonic anhydrase: new insights for an ancient enzyme. J Biol Chem *276*, 48615-48618.

Vander Heiden, M.G., Cantley, L.C., and Thompson, C.B. (2009). Understanding the Warburg effect: the metabolic requirements of cell proliferation. Science *324*, 1029-1033.

Vaupel, P., and Multhoff, G. (2021). The Warburg Effect: Historical Dogma Versus Current Rationale. Adv Exp Med Biol *1269*, 169-177.

Vemuri, G.N., Altman, E., Sangurdekar, D.P., Khodursky, A.B., and Eiteman, M.A. (2006). Overflow metabolism in Escherichia coli during steady-state growth: transcriptional regulation and effect of the redox ratio. Appl Environ Microbiol *72*, 3653-3661.

Vermes, I., Haanen, C., Steffens-Nakken, H., and Reutelingsperger, C. (1995). A novel assay for apoptosis. Flow cytometric detection of phosphatidylserine expression on early apoptotic cells using fluorescein labelled Annexin V. J Immunol Methods *184*, 39-51.

Wang, T., Marquardt, C., and Foker, J. (1976). Aerobic glycolysis during lymphocyte proliferation. Nature *261*, 702-705.

Warburg, O. (1923). Versuche an überlebendem Carcinomgewebe. Biochem Zschr *142*, 317–333.

Warburg, O. (1956). On the origin of cancer cells. Science *123*, 309-314.

Weinberg, R.A. (1995). The retinoblastoma protein and cell cycle control. Cell *81*, 323-330.

You, H., Stephenson, R.J., Gobert, G.N., and McManus, D.P. (2014). Revisiting glucose uptake and metabolism in schistosomes: new molecular insights for improved schistosomiasis therapies. Front Genet *5*, 176.

Zeng, W.P., McFarland, M.M., Zhou, B., Holtfreter, S., Flesher, S., Cheung, A., and Mallick, A. (2017). Staphylococcal enterotoxin A-activated regulatory T cells promote allergen-specific TH2 response to intratracheal allergen inoculation. J Allergy Clin Immunol *139*, 508-518 e504.

Ziv, N., Brandt, N.J., and Gresham, D. (2013). The use of chemostats in microbial systems biology. J Vis Exp.

Acknowledgments

WZ thanks Dr. Tiru Rangasamy for technical information regarding sensitization and challenge of mice with OVA**.**

Author Contribution

WZ conceived, designed and carried out the study, and wrote the manuscript.

Competing interest

WZ is the inventor of a patent application based in part on some data presented in this article.

Data and materials availability

All data are available in the manuscript.

Figures and Legends

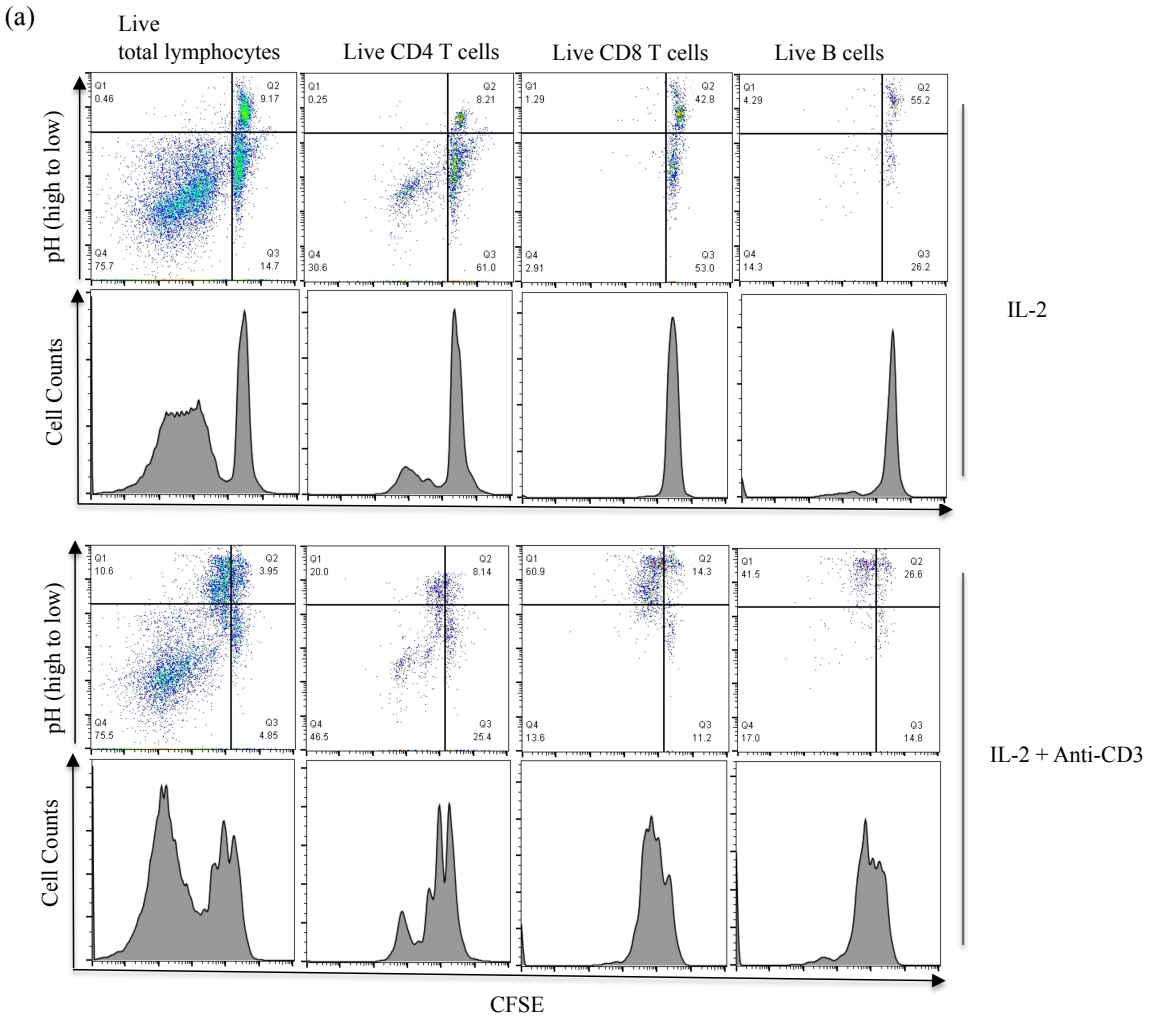

Fig. 1. Positive correlation between intracellular pH and lymphocyte proliferation.

(a) CFSE-labeled lymph node cells stimulated in vitro with IL-2, or IL-2 and anti-CD3 antibodies. Shown are flow cytometric pseudocolor plots of CFSE signals and intracellular pH, and histograms of CFSE signals of live total lymphocytes, CD4, CD8 T cells and B cells.

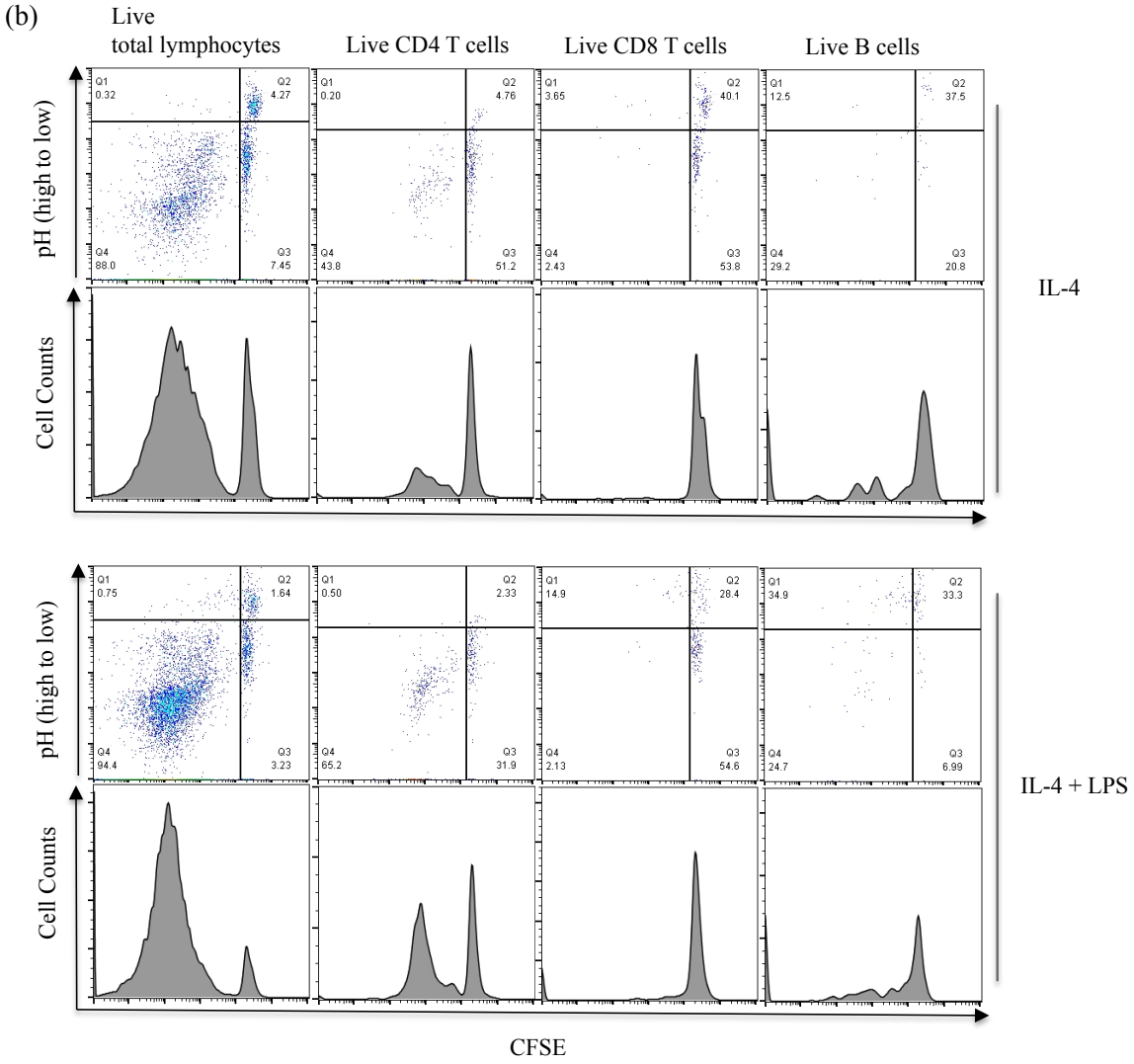

Fig. 1 (b) CFSE-labeled lymph node cells stimulated in vitro with IL-4 or IL-4 and LPS.

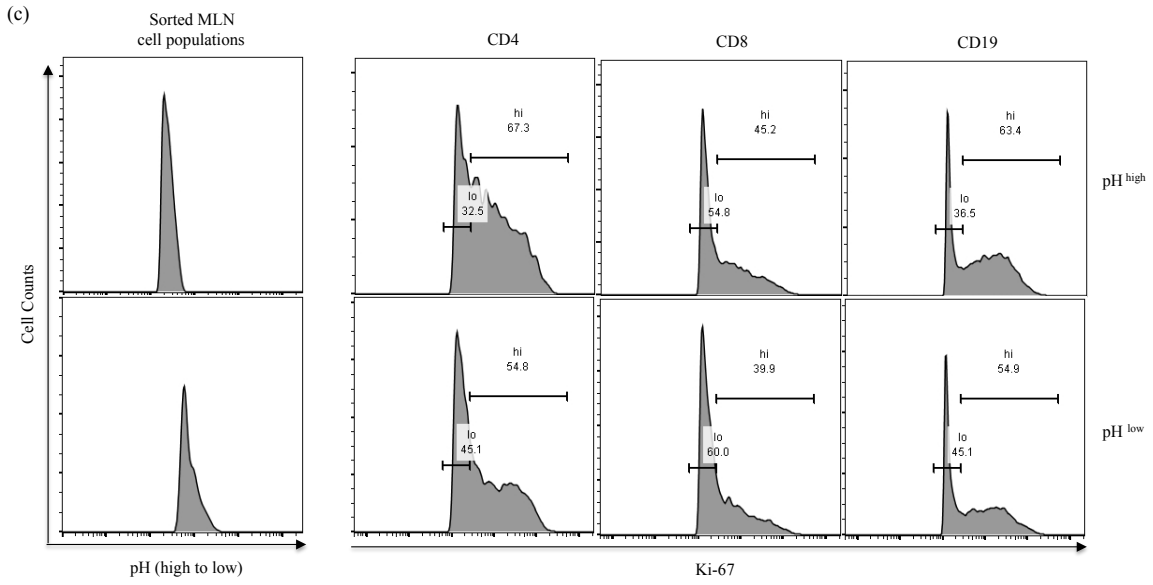

Fig. 1 (c) Draining lymph node cells of in vivo immune response. OVA-sensitized mice were i.t. challenged with OVA every other day for 3 time, and MLNs were harvested 7 days after the initial challenge. Live MLN cells were sorted into pH high and low populations. Left panels are the histograms of the intracellular pH profiles of the sorted populations. Right panels are histograms of Ki-67 expression showing the percentages of Ki-67 high and low cells in the proliferating CD4, CD8 T cells and B cells ($CD19^{+}$) of the sorted populations.

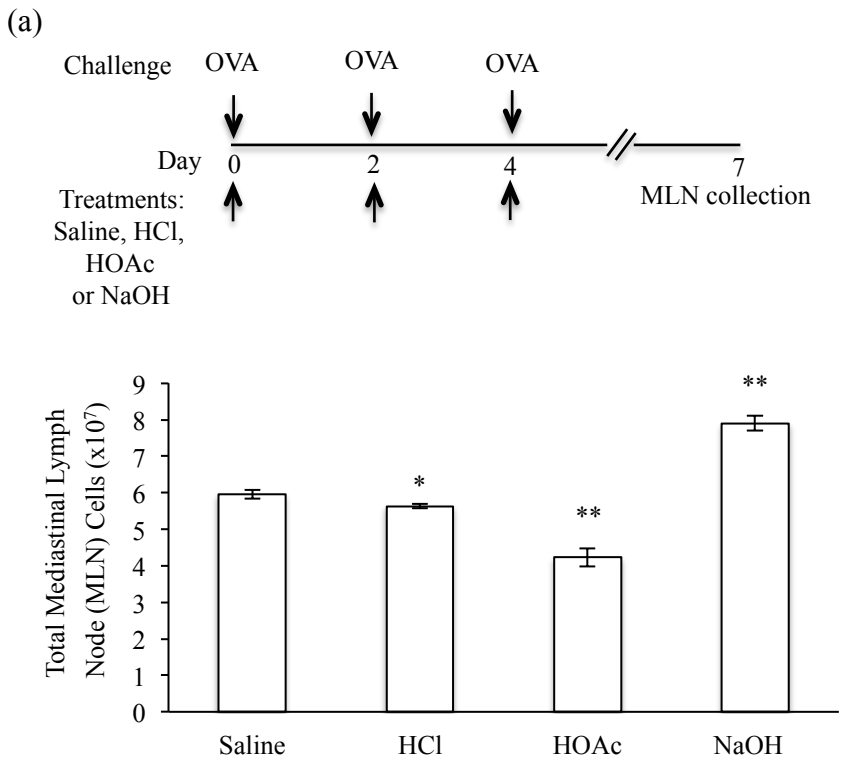

Fig. 2. Effects of pH modifiers on the populations and proliferation of lymphocytes in MLNs. (a) Total numbers of MLN cells. Upper: Schematic illustration of the schedules for OVA challenges and treatments with saline, or saline plus HCl, HOAc or NaOH of the OVA-sensitized mice. Arrows indicate the time points for the challenges or treatments. Lower: A graph showing the average total numbers of MLN cells of mice in the different treatment groups. Statistical significance between the saline and the other groups was determined by Student t test; * $p < 0.05$, ** $p < 0.01$.

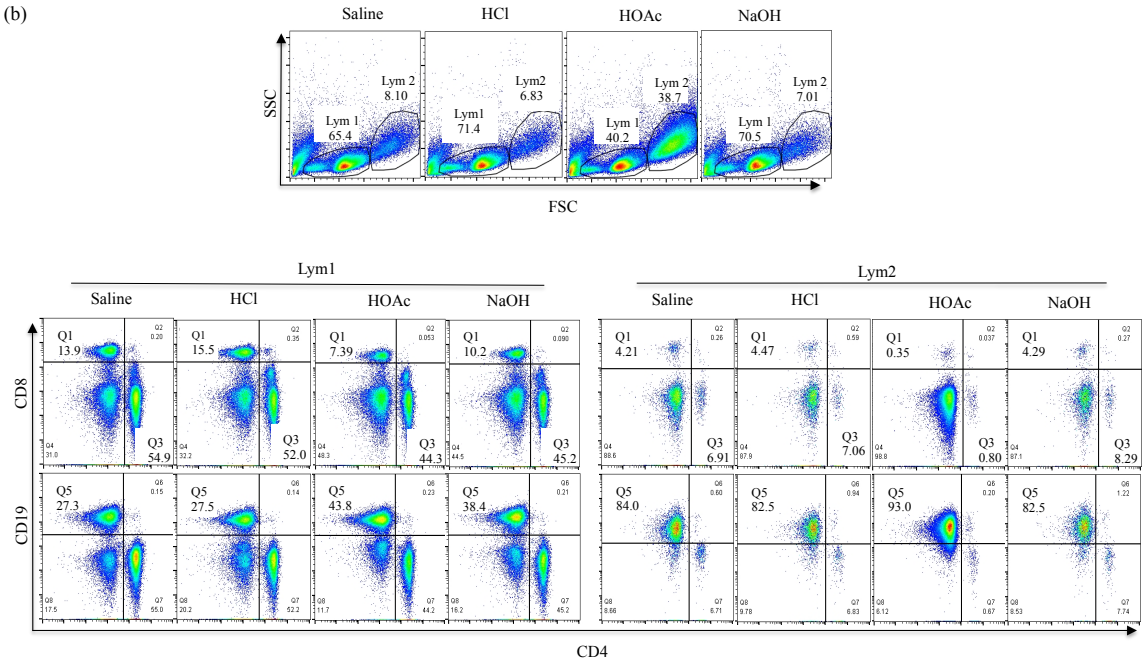

Fig. 2 (b) Lymphocyte populations in the MLNs. The upper panels are flow cytometry plots showing the Lym1 and Lym2 lymphocyte populations in live MLN cells of the different treatment groups. The lower panels show the populations of CD4, CD8 T cells and B cells ($CD19^{+}$) in Lym1 and Lym2. Numbers in the plots are the percentages of each cell populations.

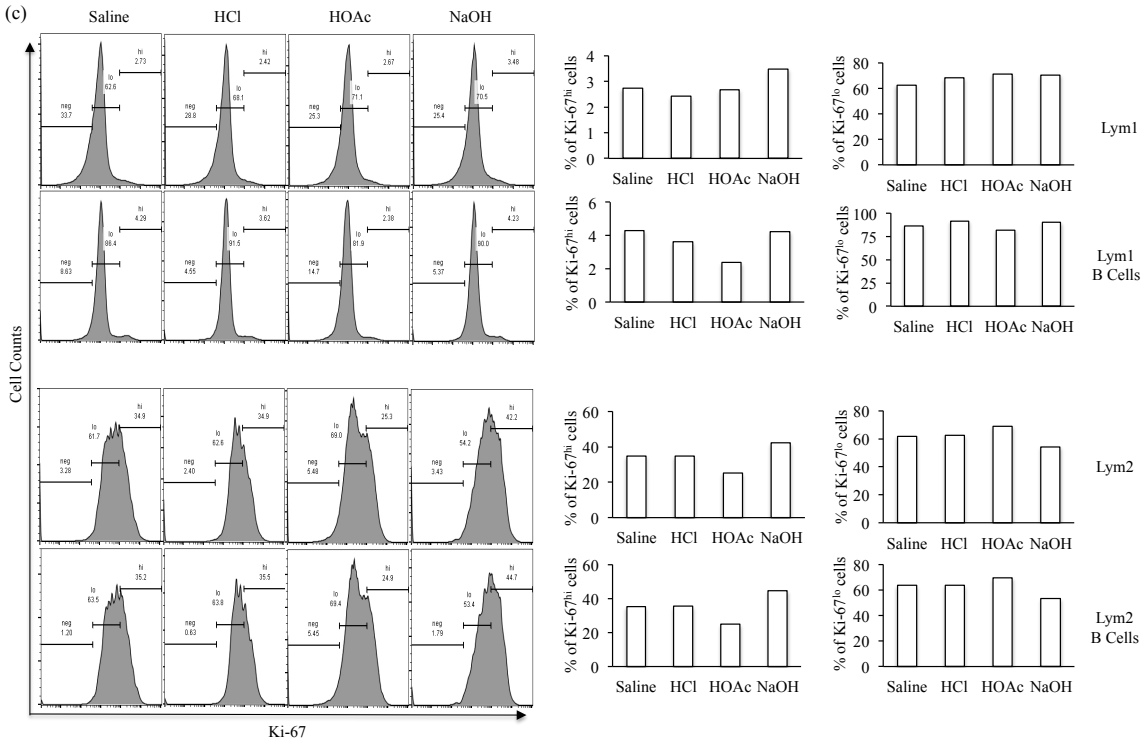

Fig. 2 (c) Expression of Ki-67. Left panels are histograms showing Ki-67 expression, and the percentages of Ki-67 high, low negative cells in Lym1, Lym2 and B cells thereof. Right panels are graphic presentation of the percentages of the Ki-67 high and low cells in the left panels.

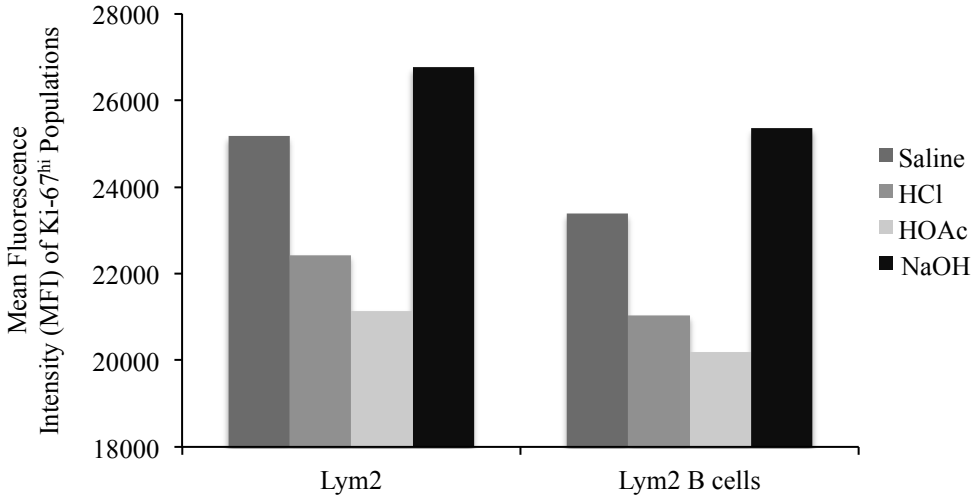

Fig. 2 (d) Mean fluorescence intensities of Ki-67^{hi} cells in the Lym2 populations and their B cells of the different treatment groups.

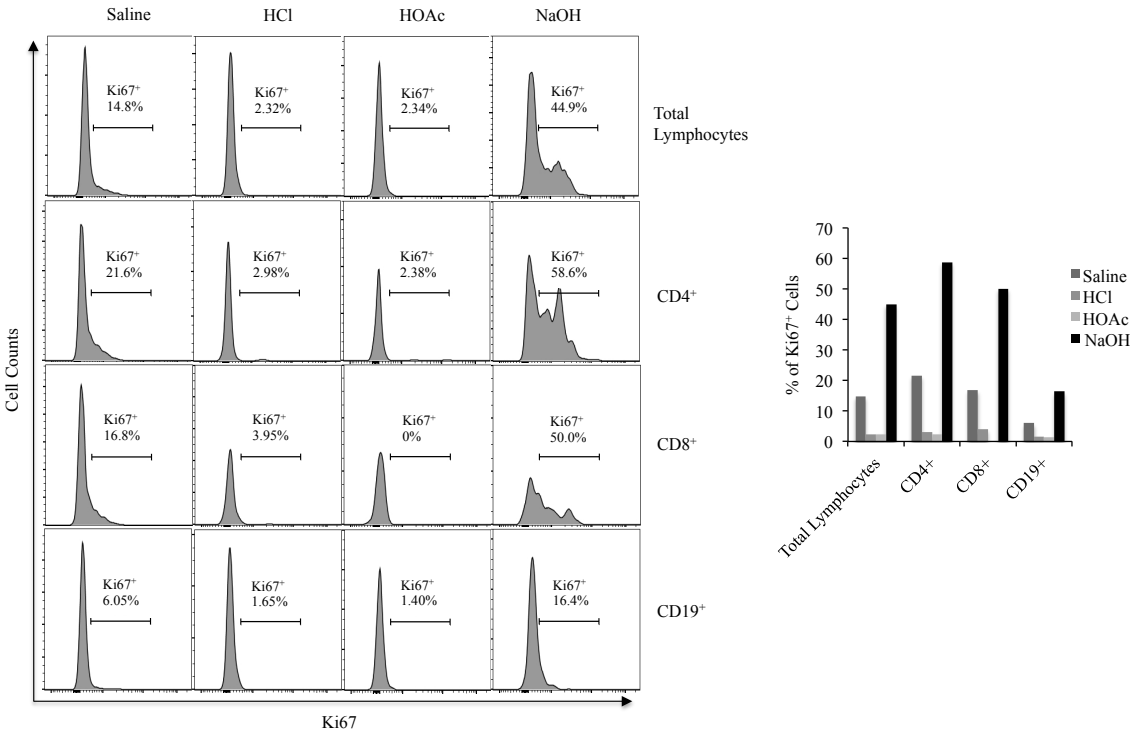

Fig. 3. Effects of in vitro treatments with pH modifiers on lymphocyte proliferation. Primary lymph node cells were incubated in FBS containing 10% saline or saline plus HCl, HOAc or NaOH, then analyzed by flow cytometry to determine Ki-67 expression in live total lymphocytes, CD4, CD8 T cells and B cells ($CD19^+$). Left panels are histograms of Ki-67 expression in the different lymphocyte populations. Right panel is graphic presentation of the percentages of Ki-67^+ cells in the left panels.

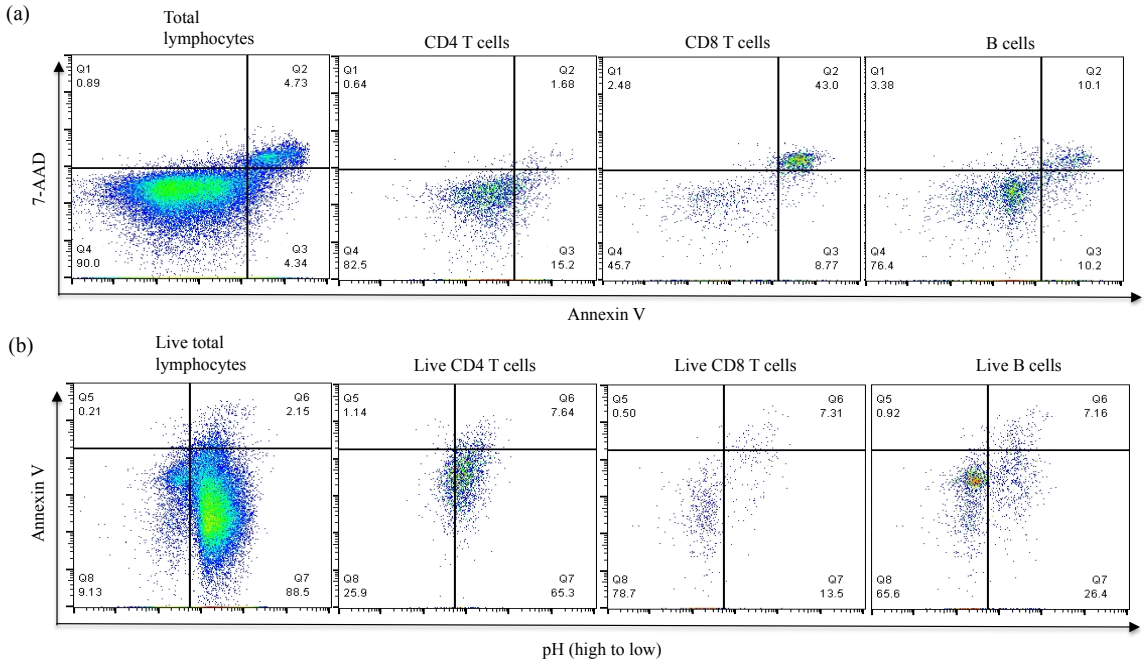

Fig. 4. Relation between low intracellular pH and lymphocyte apoptosis. Total lymphocytes, CD4, CD8 T cells and B cells under different experimental conditions as indicated were analyzed by flow cytometry for the staining of Annexin V, 7AAD or Zombie-violet, and the pH indicator pHrodo^{TM} Green.

(a, b) Steady-state peripheral lymphocytes of unimmunized mice.

(a) Plots showing the staining of Annexin V and 7AAD in the different lymphocytes. Cells in the Q2 quadrants (Annexin V^{hi} 7AAD^{+}) are apoptotic cells, and cells in the Q3 quadrants (Annexin V^{hi} 7AAD$^{-)}$ are early apoptotic cells.

(b) Plots showing the staining of the pH indicator and Annexin V in the live (7AAD^{-}) populations of the different lymphocytes as indicated.

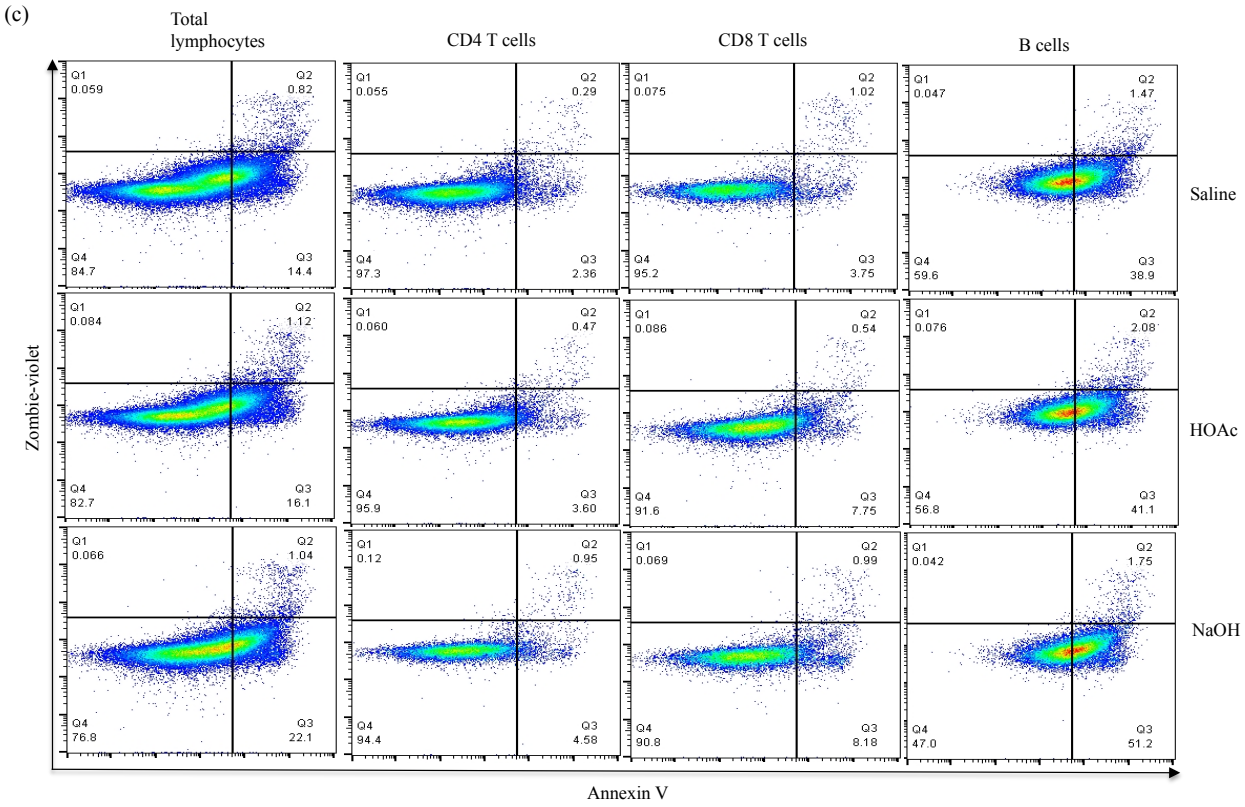

Fig. 4 (c, d, e) Ex vivo MLN cells of OVA-sensitized and challenged mice that were treated with saline or saline plus HOAc or NaOH.

(c) Plots showing the staining of Annexin V and Zombie-violet of the different lymphocytes as indicated.

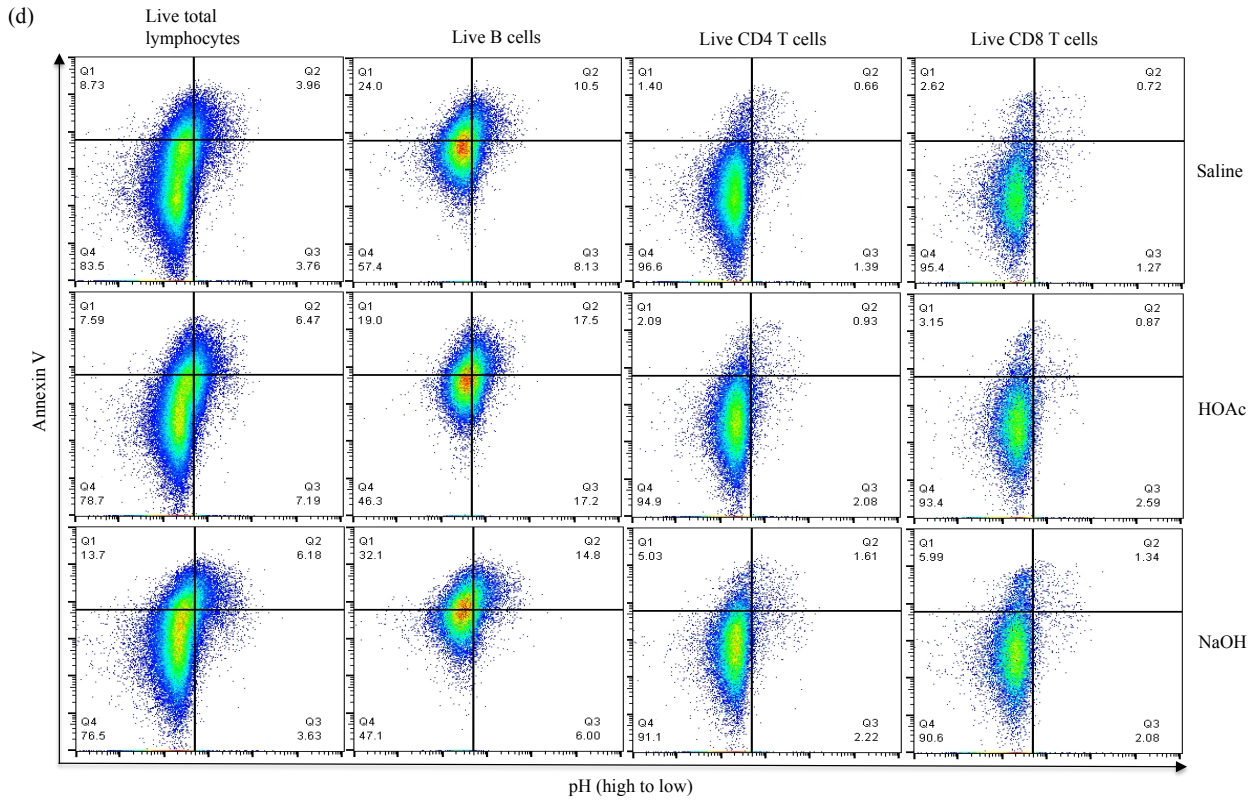

Fig. 4 (d) Plots showing the staining of Annexin V and the pH indicator in the live populations (Zombie-violet^{-}) of the different lymphocytes.

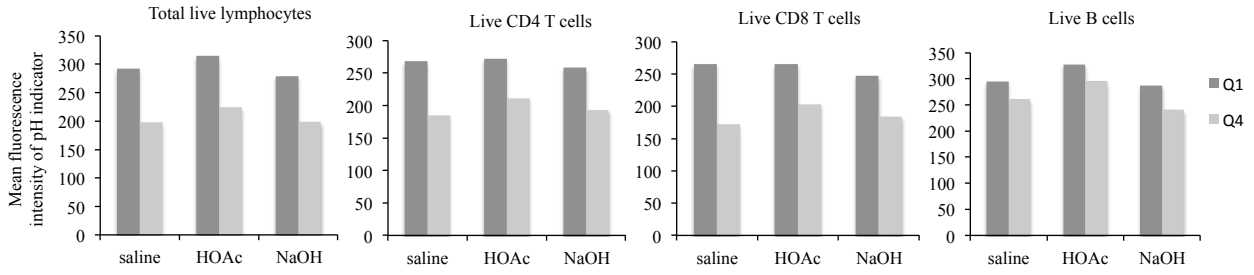

Fig. 4 (e) Bar graphs showing the mean fluorescence intensities (MFI) of pHrodo^{TM} Green staining of the early apoptotic (Annexin V^{hi}) cells (Q1) and the non-apoptotic (Annexin V^{lo}) cells (Q4) within the overall pH high cells in (d).

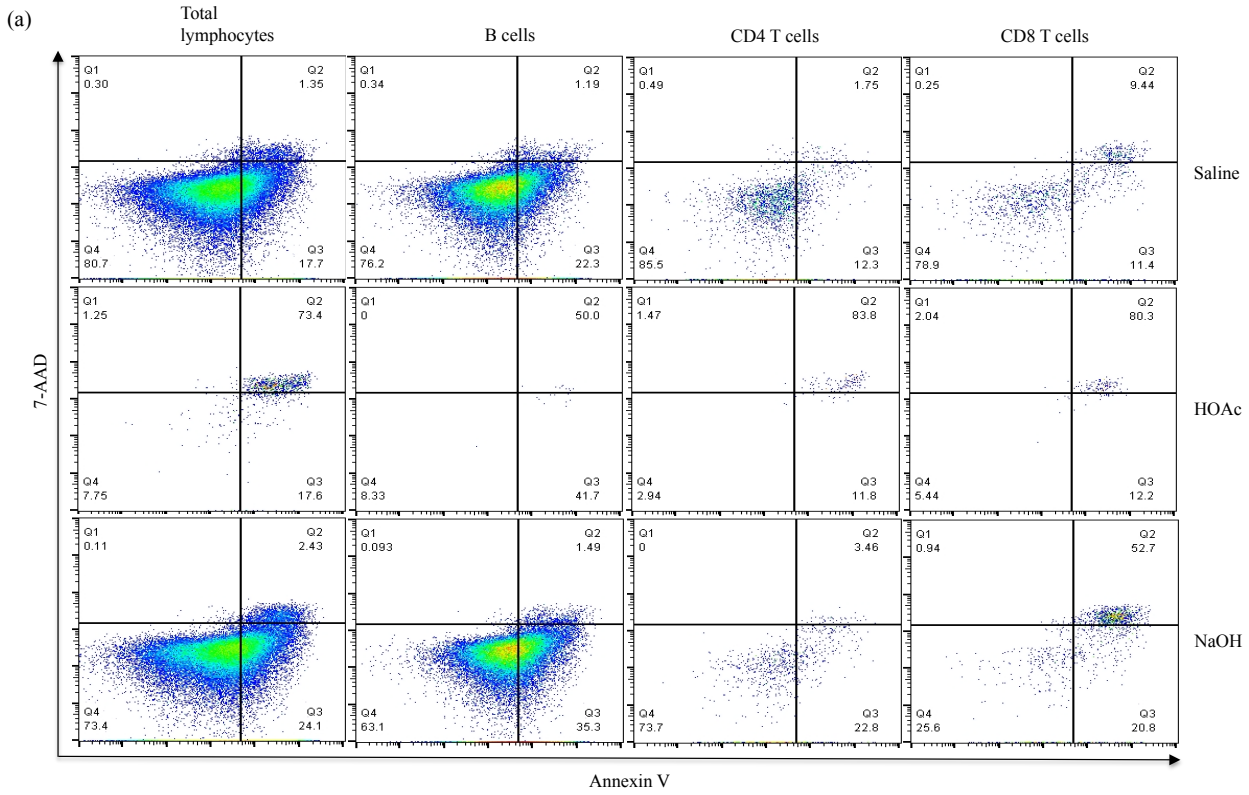

Fig. 5. Effects of in vitro treatments with pH modifiers on apoptosis of the MLN lymphocytes. MLN cells from mice that were sensitized and challenged with OVA were treated in vitro with saline or saline plus HOAc or NaOH in FBS.

(a) Plots showing the staining of 7AAD and Annexin V in total lymphocytes, CD4, CD8 T cells and B cells in the different treatment groups.

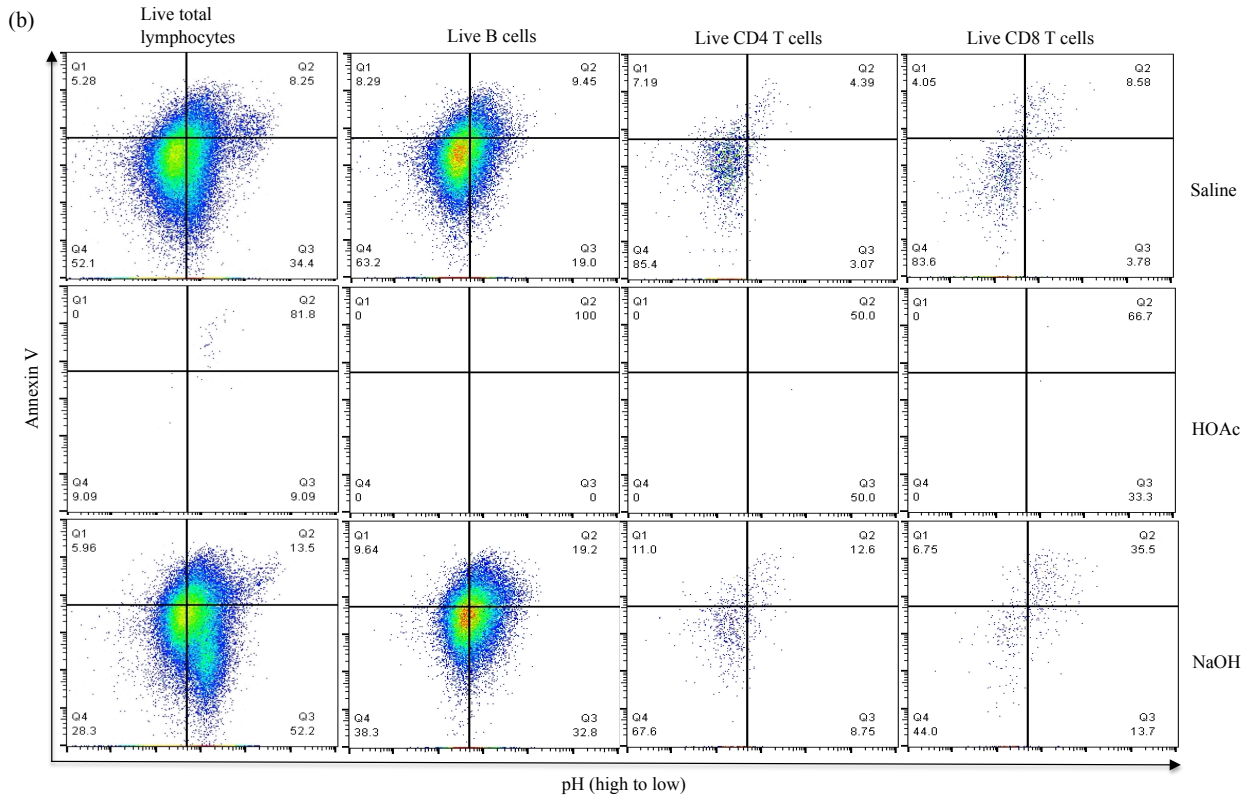

Fig. 5 (b) Plots showing the staining of the pH indicator pHrodo^{TM} Green and Annexin V in the live total lymphocytes, CD4, CD8 T cells and B cells.

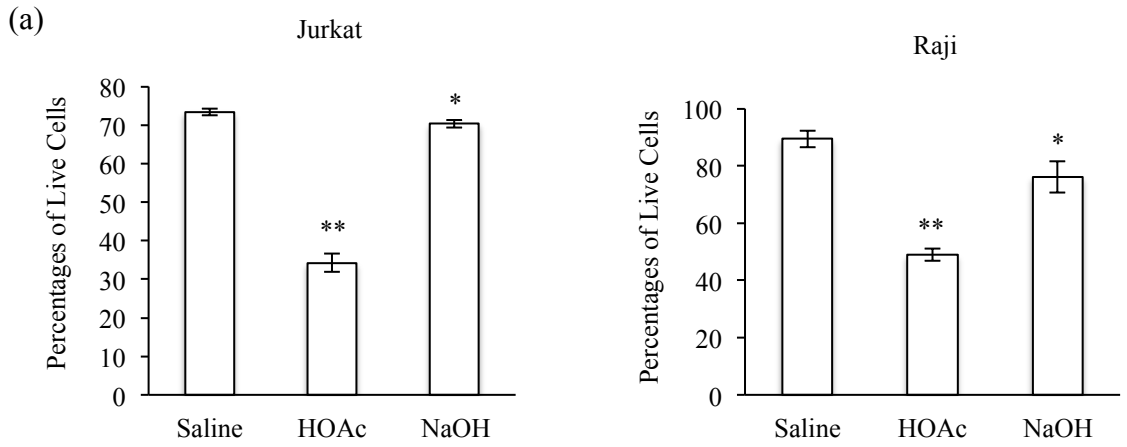

Fig. 6. Effects of pH modifiers on the proliferation and apoptosis of tumor cells.

(a) Comparison of the average viabilities of Jurkat and Raji cells as determined by Trypan Blue staining after treatments with saline or saline plus HOAc or NaOH in FBS. Statistical significance of differences between the saline and other treatment groups was determined by Student t test, * $p < 0.05$, ** $p < 0.01$.

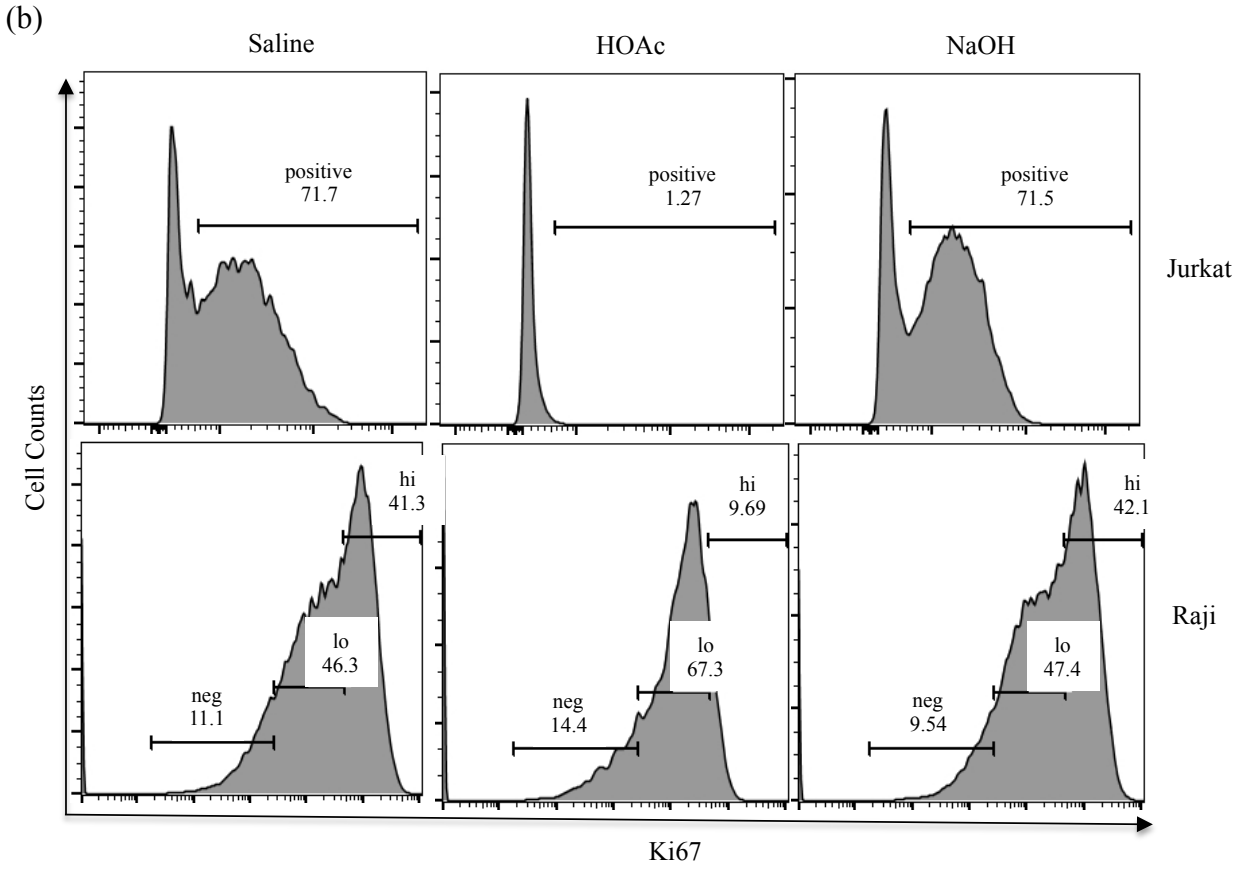

Fig. 6 (b) Histograms of Ki-67 staining in live Jurkat or Raji cells after the different treatments. The numbers in the histograms are the percentages of each population defined by their levels of Ki-67 staining.

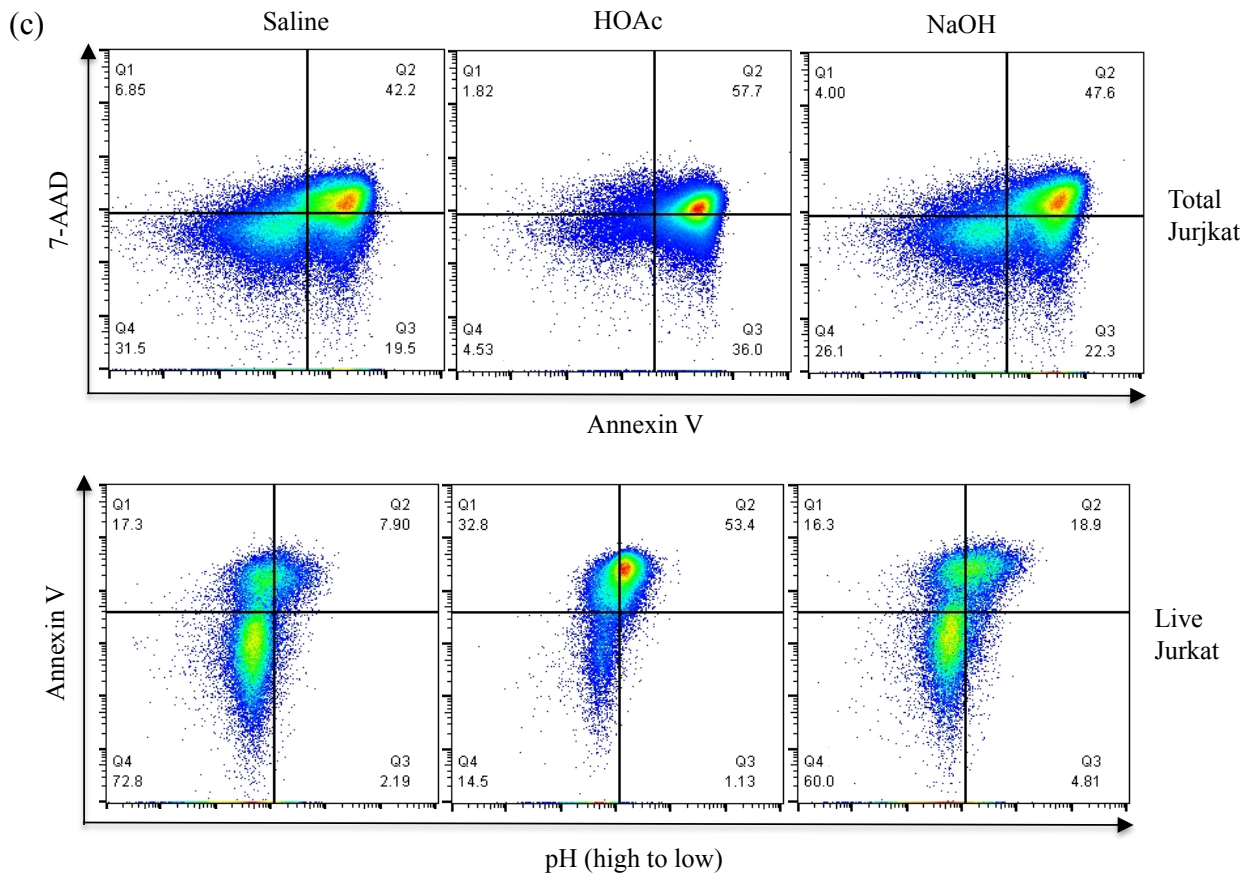

Fig. 6 (c) Apoptosis of Jurkat cells. Upper panels show the staining of 7AAD and Annexin V of Jurkat cells after the different treatments. Lower panels show the staining of the pH indicator pHrodo^{TM} Green and Annexin V in live (7AAD^{-}) Jurkat cells after the treatments.

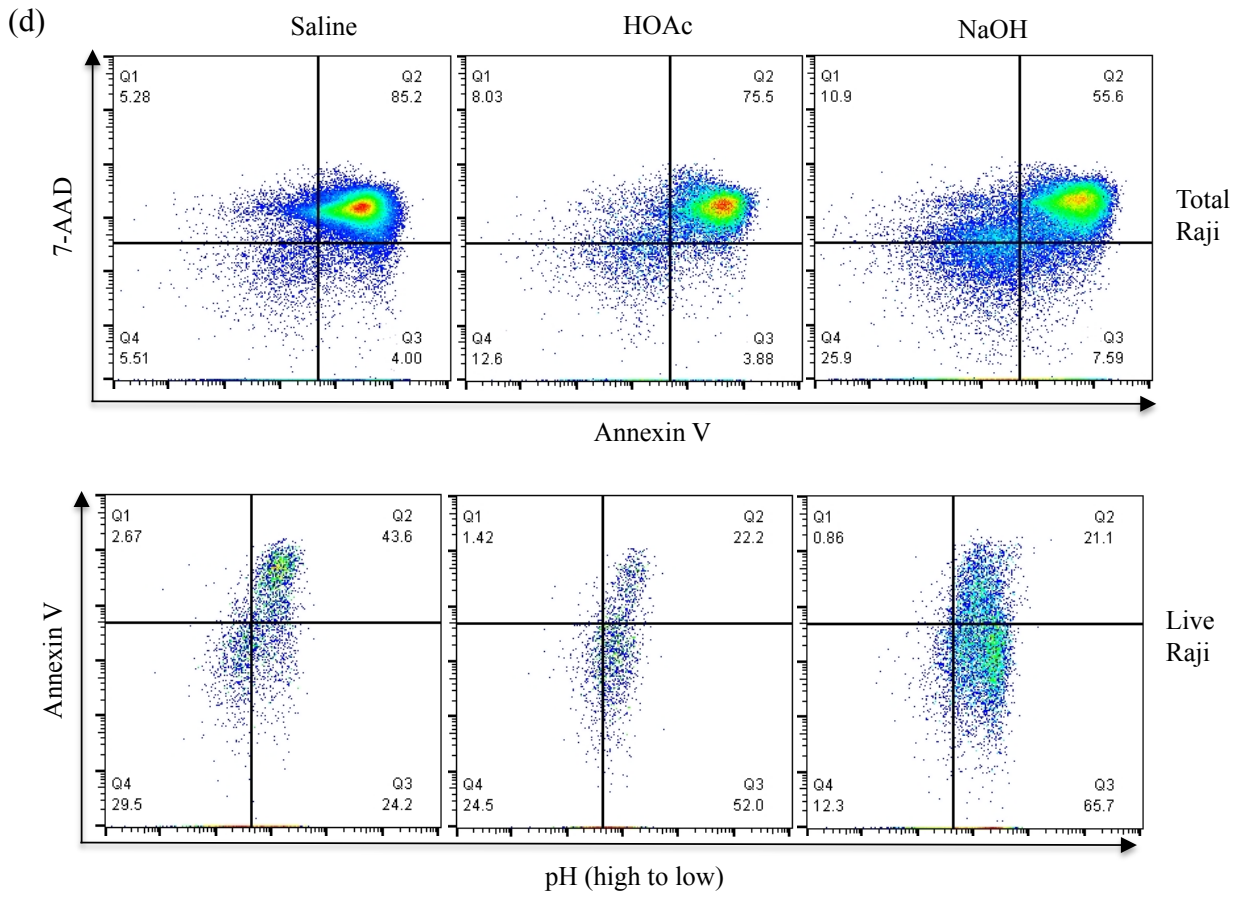

Fig. 6 (d) Apoptosis of Raji cells. Upper panels show the staining of 7AAD and Annexin V of Raji cells after the different treatments. Lower panels show the staining of the pH indicator and Annexin V in live Raji cells after the treatments.

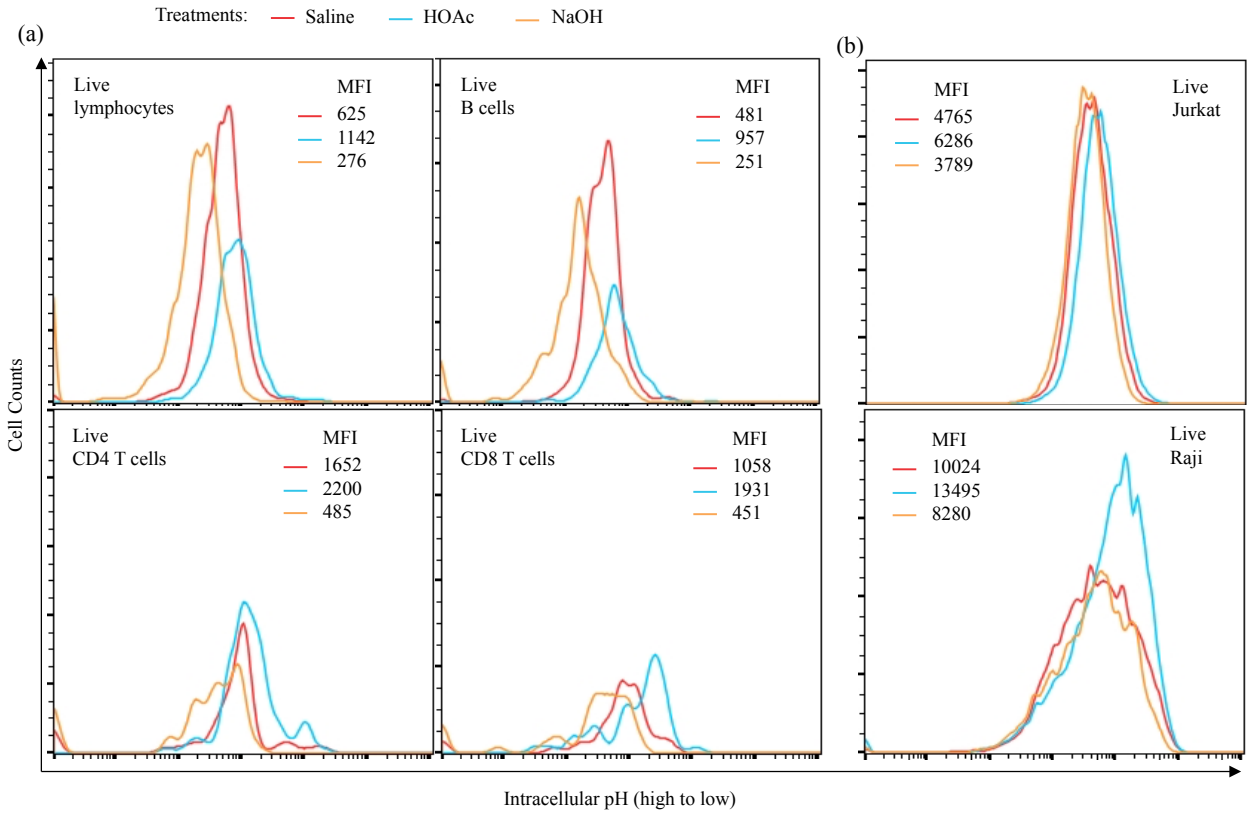

Fig. 7. Alteration of intracellular pH by treatments with pH modifiers.

(a) MLN cells of OVA-sensitized and challenged mice. Sensitizations, challenges and MLN collection were carried out as in Fig. 1c. MLN cells were treated in vitro with saline, or saline plus HOAc or NaOH in FBS as indicated. Shown are overlays of histograms of intracellular pH of the different live lymphocyte populations after the different treatments. MFI: mean fluorescence intensity of pHrodo^{TM} Green staining.

(b) Jurkat and Raji cells. Shown are overlays of histograms and MFI of intracellular pH indicator after the different treatments.

Supplemental Information

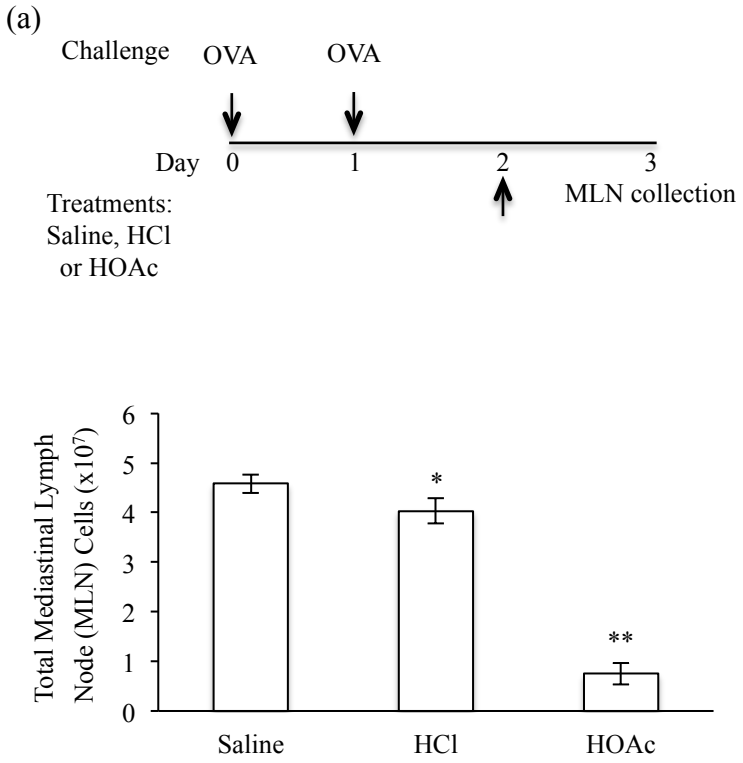

Suppl. Fig. 1. Effects of pH modifiers on the populations and proliferation of lymphocytes in MLNs 3 days after initial OVA challenge.

(a) The top panel is a schematic illustrating the schedules for OVA challenges and treatments with saline, or saline plus HCl or HOAc of OVA-sensitized mice. Arrows indicate the time points for the challenges or treatments. The lower panel shows the average total numbers of MLN cells of mice in the different treatment groups. Statistical significance between saline and the other groups was determined by Student t test; * $p < 0.05$, ** $p < 0.01$.

(b)

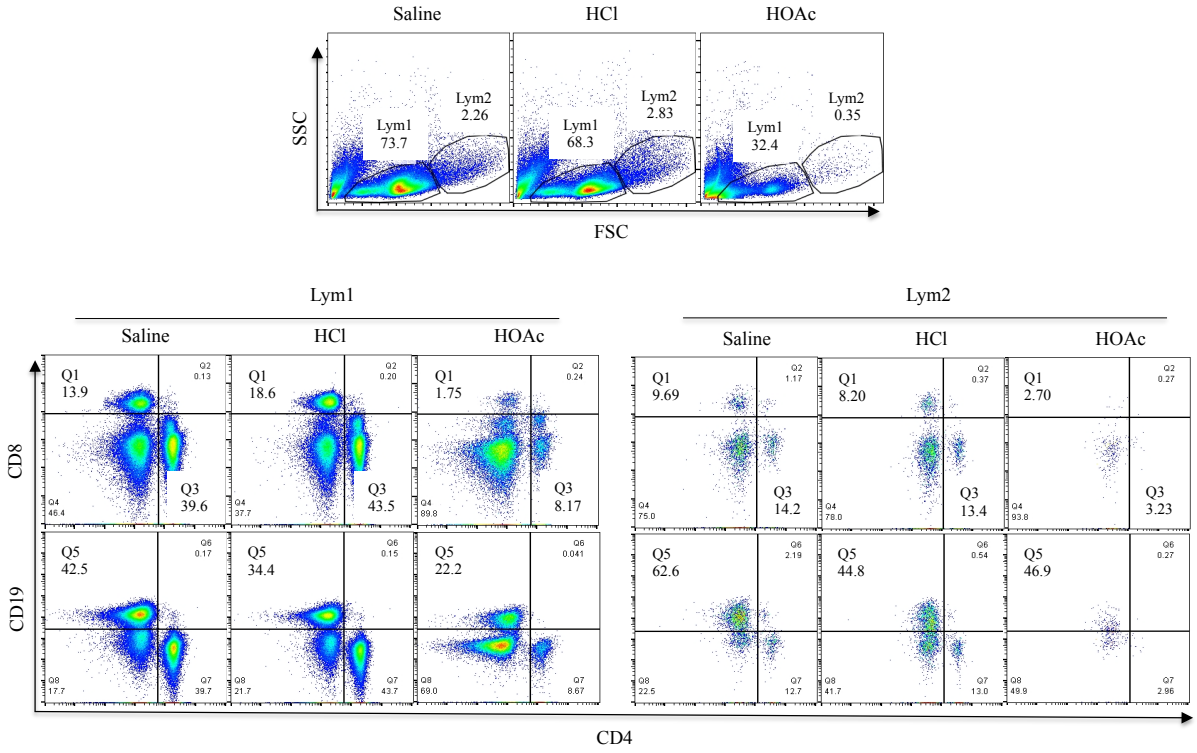

Suppl. Fig. 1 (b) The upper panels show the Lym1 and Lym2 lymphocyte populations in the MLNs of the different treatment groups. The lower panels show the populations of CD4, CD8 T cells and B cells ($CD19^{+}$) in the Lym1 and Lym2 lymphocytes. Numbers in the plots are the percentages of each cell populations.

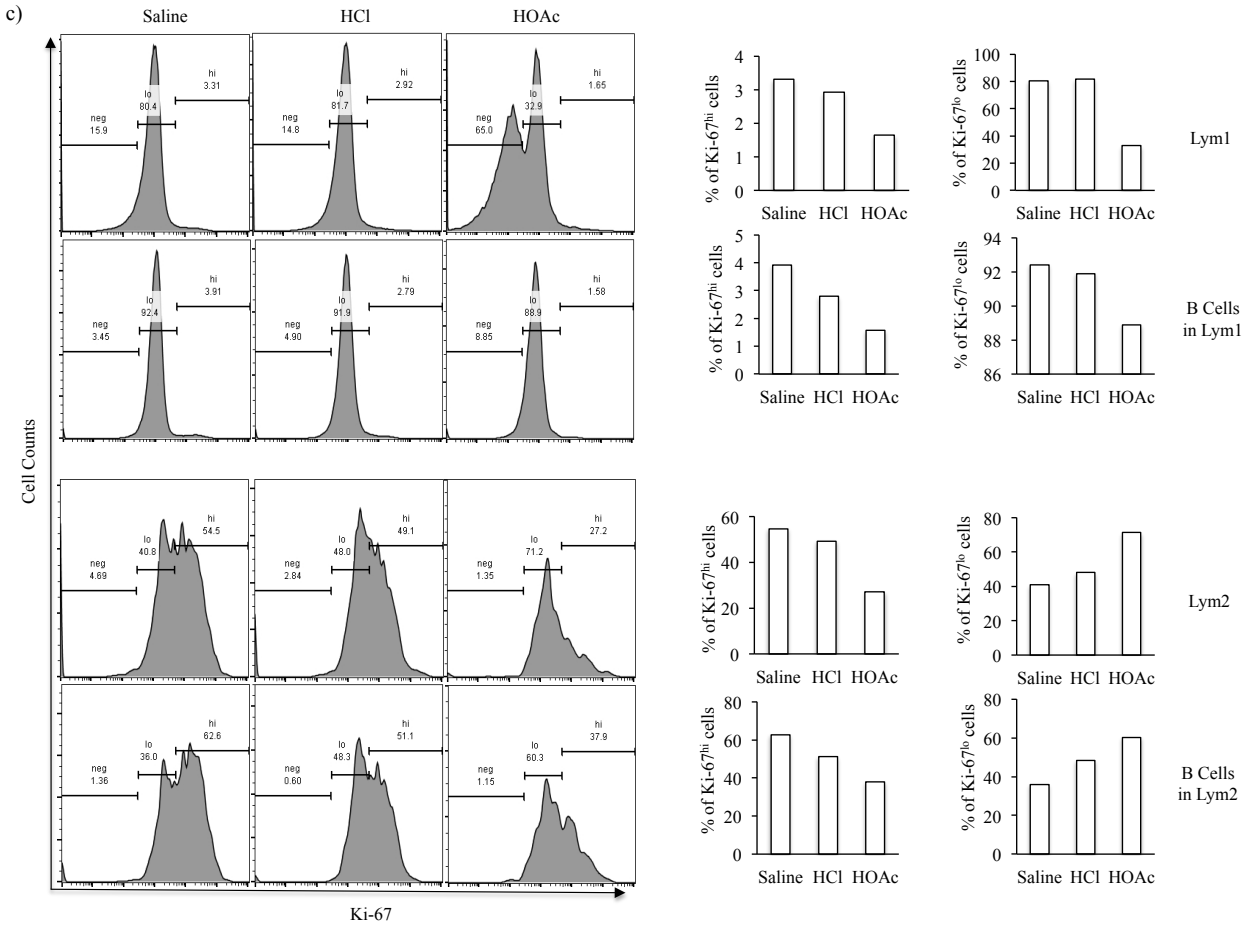

Suppl. Fig. 1 (c) Expression of Ki-67. Left panels are histograms showing Ki-67 expression, and percentages of Ki-67 high, low negative cells in Lym1, Lym2 and the B cells thereof. Right panels are graphic presentation of the percentages of the Ki-67 high and low cells.

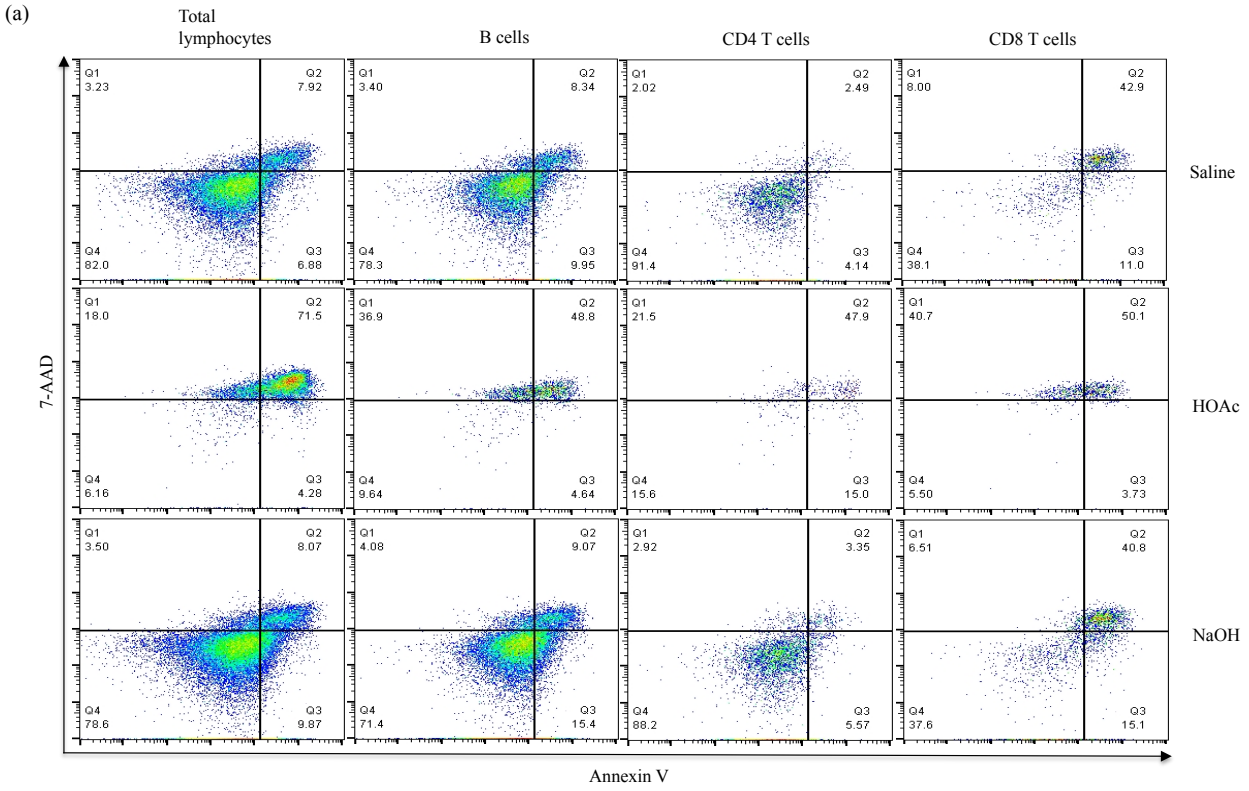

Suppl. Fig. 2. Correlation between low pH and apoptosis of in vitro cultured lymphocytes. After mitogenic stimulation, the cells were treated with saline or saline plus HOAc or NaOH in FBS, then stained with intracellular pH indicator pHrodo^{TM} Green, Annexin V, and 7-AAD.

(a, b) Lymphocytes stimulated with anti-CD3 plus IL-2.

(a) Pseudocolor plots of Annexin V and 7AAD staining of the different lymphocyte populations of the different treatment groups as indicated.

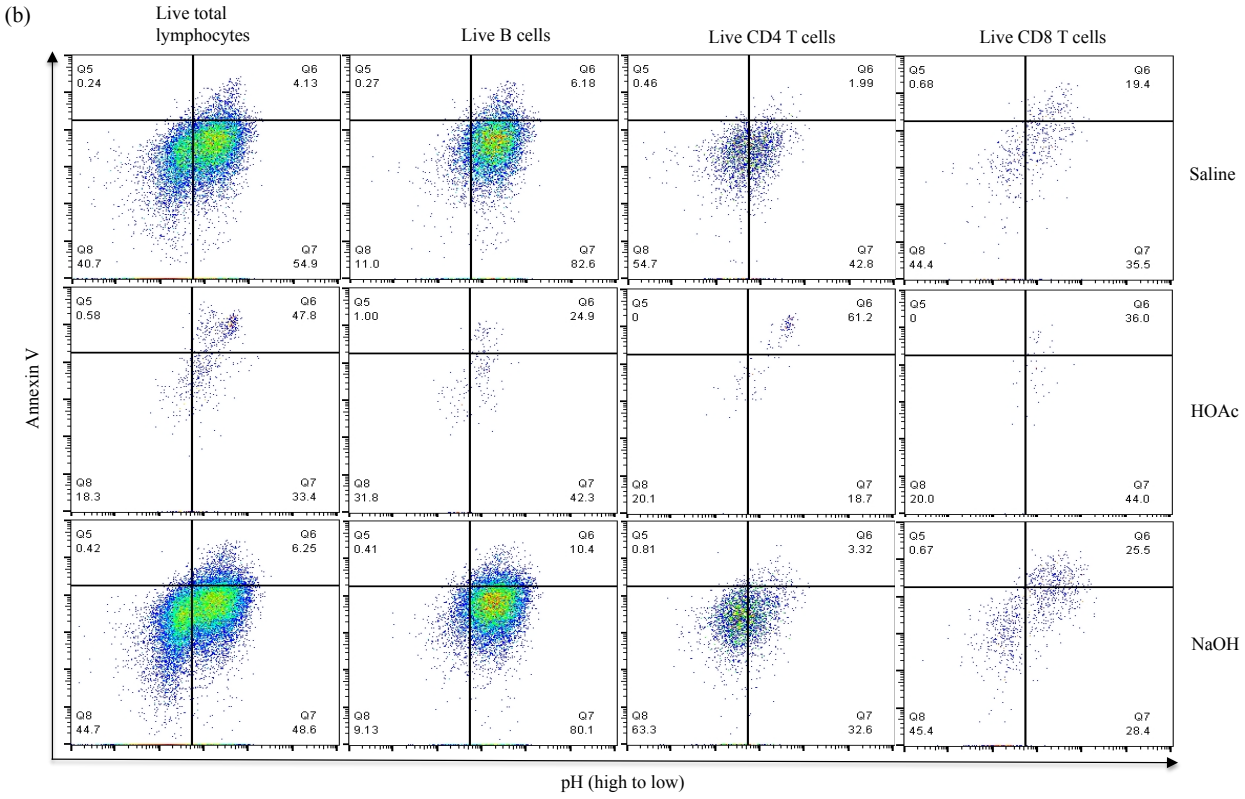

Suppl. Fig. 2 (b) Pseudocolor plots of pH indicator and Annexin V staining in the different live (7AAD$^-$) lymphocyte populations and treatment groups.

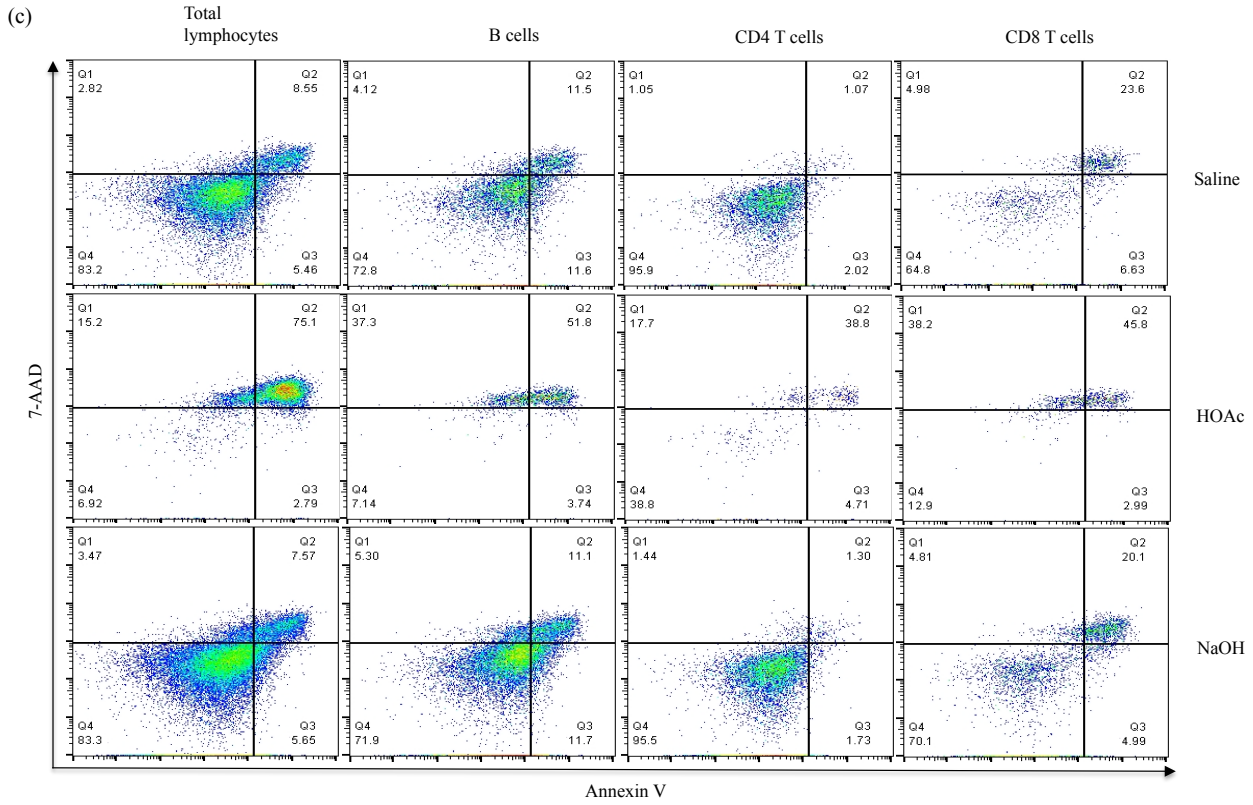

Suppl. Fig. 2 (c, d) Lymphocytes stimulated with LPS plus IL-4.

(c) Plots showing Annexin V and 7AAD staining in the different lymphocyte populations and treatment groups.

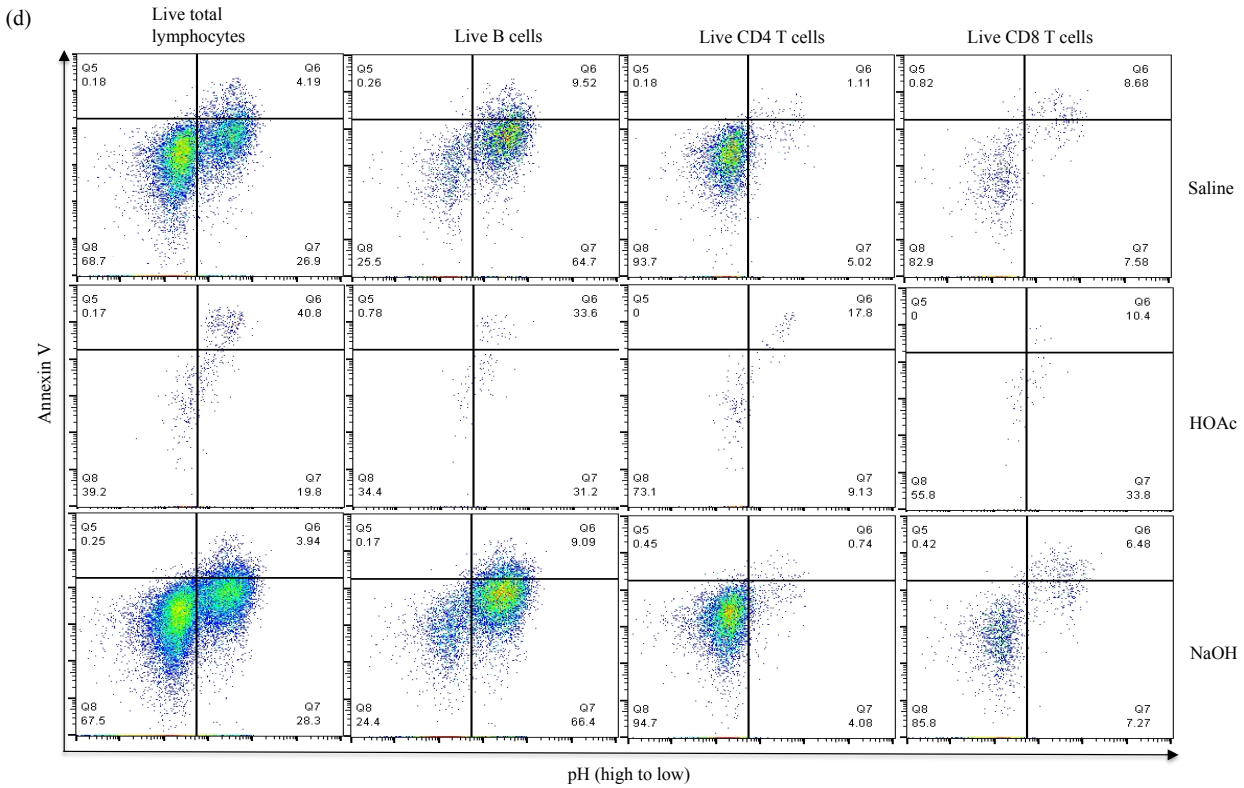

Suppl. Fig. 2 (d) Plots showing the pH indicator and Annexin V staining in the different live (7AAD$^-$) lymphocyte populations and treatment groups.

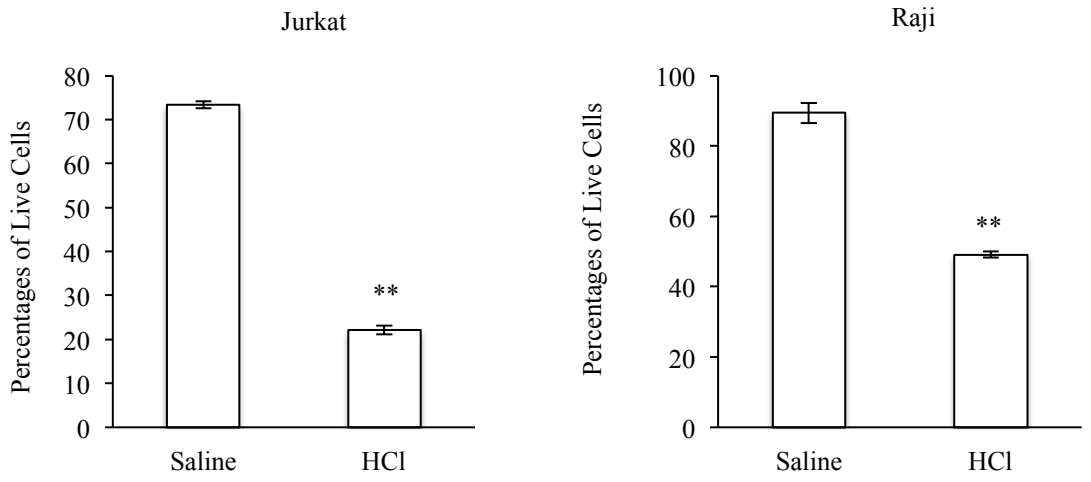

Suppl. Fig. 3. Comparisons of tumor cell viabilities after treatment with saline or saline plus HCl in FBS. Shown are average viabilities of Jurkat and Raji cells determined by Trypan Blue staining in the different treatment groups as indicated. Statistical significance of differences between the saline and HCl treatment groups was determined by Student t test, ** $p < 0.01$.